

Review

Uranium and Fluoride Removal from Aqueous Solution Using Biochar: A Critical Review for Understanding the Role of Feedstock Types, Mechanisms, and Modification Methods

Anjali Thakur¹, Rakesh Kumar²  and Prafulla Kumar Sahoo^{1,3,*}

¹ Department of Environmental Science and Technology, Central University of Punjab, V.P.O. Ghudda, Bathinda 151401, Punjab, India

² School of Ecology and Environment Studies, Nalanda University, Rajgir 803116, Bihar, India

³ Instituto Tecnológico Vale (ITV), Rua Boaventura da Silva, 955, Belém 66055-090, PA, Brazil

* Correspondence: prafulla.iitkgp@gmail.com

Abstract: Uranium (U) and fluoride (F⁻) are the major global geogenic contaminants in aquifers and pose serious health issues. Biochar, a potential adsorbent, has been widely applied to remediate geogenic and anthropogenic contaminants. However, there is a lack of research progress in understanding the role of different feedstock types, modifications, adsorption mechanisms on physico-chemical properties of biochar, and factors affecting the adsorption of U and F⁻ from aqueous solution. To fill this lacuna, the present review gives insight into the U and F⁻ removal from aqueous solution utilizing biochar from various feedstocks. Feedstock type, pyrolysis temperature, modifications, solution pH, surface area, and surface-charge-influenced biochar adsorption capacities have been discussed in detail. Major feedstock types that facilitated U and F⁻ adsorption were crop residues/agricultural waste, softwood, grasses, and animal manure. Low-to-medium pyrolyzing temperature yielded better biochar properties for U and F⁻ adsorption. Effective modification techniques were mainly acidic and magnetic for U adsorption, while metal oxides, hydroxides, alkali, and magnetic modification were favourable for F⁻ adsorption. The major mechanisms of U adsorption were an electrostatic attraction and surface complexation, while for F⁻ adsorption, the major mechanisms were ion exchange and electrostatic attraction. Lastly, the limitations and challenges of using biochar have also been discussed.

Keywords: biochar; uranium; fluoride; adsorption mechanism; feedstocks; aqueous solution; remediation



Citation: Thakur, A.; Kumar, R.; Sahoo, P.K. Uranium and Fluoride Removal from Aqueous Solution Using Biochar: A Critical Review for Understanding the Role of Feedstock Types, Mechanisms, and Modification Methods. *Water* **2022**, *14*, 4063. <https://doi.org/10.3390/w14244063>

Academic Editors: Gaurav Sharma and Saglara S. Mandzhieva

Received: 23 October 2022

Accepted: 4 December 2022

Published: 13 December 2022

Publisher's Note: MDPI stays neutral with regard to jurisdictional claims in published maps and institutional affiliations.



Copyright: © 2022 by the authors. Licensee MDPI, Basel, Switzerland. This article is an open access article distributed under the terms and conditions of the Creative Commons Attribution (CC BY) license (<https://creativecommons.org/licenses/by/4.0/>).

1. Introduction

Rapid industrialization, rising population, unplanned urbanization, and intense agricultural activities have severely exploited water resources. As a result, the demand for clean water has increased tremendously. According to the United Nations Children's fund (UNICEF) and World Health Organization (WHO) report, about 2.2 billion people globally and up to 600 million people in underdeveloped nations still lack access to clean water [1]. Goal 6 of the United Nations (UN) Sustainable Development Goals (SDGs) seeks to ensure access to water and sanitation for all, implying the need to improve water quality and protect water-related ecosystems. This goal points to the need for synthesizing technological advances in water research to be economically viable for developing countries [2]. Groundwater serves as the primary supply of drinking water in the majority of the developing nations due to inadequate freshwater sources. However, groundwater contamination has recently increased due to several contaminants (As, U, F⁻, Cd, Cr, Zn, NO₃⁻, PO₄³⁻, etc.) via geogenic and endless anthropogenic activities [3,4]. Among them, U and F⁻ contamination is mainly caused by geogenic sources [5]. The intake of higher levels of U and F⁻ can cause serious health issues such as nephrotoxicity, dental and skeletal fluorosis, bone cancer, and brain damage [6,7]; hence, it is essential to mitigate them. Elevated levels

of U in groundwater have been reported in many parts of the world, such as Finland, Greece, Germany, Australia, Canada, and the U.S., and Southeast Asian countries such as India, Pakistan, China, and Bangladesh [8]. The WHO guideline for U in drinking water is $30 \mu\text{g L}^{-1}$ and by the Atomic Energy Regulatory Board (AERB) is $60 \mu\text{g L}^{-1}$. Drinking water above these contamination limits can cause serious health issues. The health risk of U in groundwater is more due to its chemical toxicity than the radiotoxicity. Chemical toxicity causes damage to the kidney (nephrotoxicity), liver, reproductive system, and skeleton, whereas radiotoxicity targets the lungs, bones, and brain [8–10]. Globally, many nations, including India, China, Sri Lanka, Argentina, South Africa, UK, Pakistan, etc., have significant F^- concentrations in their groundwater [11,12]. More than 200 million individuals worldwide drink water with elevated F^- levels [13]. The World Health Organization states that 1.5 mg L^{-1} is the permissible limit for F^- in drinking water. However, excessive F^- intake causes skeletal and dental fluorosis, bone cancer, and brain damage [7].

Numerous techniques have been developed to mitigate U and F^- , namely membrane filtration methods such as nanofiltration and reverse osmosis, ion exchange, lime softening, coagulation by Fe/Al salts, and permeable reactive barriers using zerovalent iron. Adsorbents such as iron oxide, titanium dioxide, precipitation and coagulation, electrolytic defluoridation, adsorption, and electro dialysis have been utilized [14–20]. However, technologies have certain limitations, such as high installation and maintenance costs, pH dependence, high energy consumption, membrane fouling, and scaling [14,21]. Hence, these technologies are not cost-effective and cannot be applied in developing countries on a large scale. Among these methods, adsorption is the most effective and promising method for removing F^- , U, and other heavy metals from contaminated water. For F^- removal, various adsorbents have been used, such as activated alumina [22], bone char [23], activated carbon [24], metal oxides and hydroxides [25,26], zeolite [21], etc. Adsorbents, such as hematite [27], zeolite [28], activated carbon [29], diatomite [30], etc., have been applied for U removal. However, their expensive production cost makes them uneconomical. As a result, there is a huge demand for sustainable and low-cost adsorbent development.

Biochar is a solid, stable, porous, and low-cost adsorbent which is a carbonaceous material obtained from the thermal degradation of biomass, widely used for the remediation of contaminants from polluted/contaminated soil and water ecosystems [31,32]. Biochar has attained significant recognition due to its economic, sustainable, reusable, environmentally safe, and high adsorption efficiency. Evidence shows that biochar can remove various contaminants, including U and F^- [33–37]. For further enhancement in the adsorption of U and F^- , biochar has been modified with different techniques and materials, such as MnFe_2O_4 [38], FeCl_3 [39], HNO_3 [33], $\text{Al}(\text{OH})_3$ [13], H_3PO_4 [35], LaCl_3 [40], etc. However, there is enough literature available on the review of contaminant removal from aqueous solution using biochar, including organic and inorganic contaminants [41–51], heavy metals [52–63], emerging contaminants [64–67], and chemical and microbial pollutants [68]. However, there is no systematic review on the role of feedstocks on U and F^- removal by biochar from aqueous solution and its comparison with respect to different raw/pristine and modified biochars. Therefore, to the best of our knowledge, this review gives a systematic idea about the role of feedstock types on biochar properties, modification techniques to enhance adsorption capacity, interactions with contaminants, and factors affecting the adsorption efficiency of U and F^- removal in aqueous solution.

The present review work aims to highlight (i) the application of biochars obtained from different feedstocks for U and F^- adsorption, (ii) the different production techniques for synthesis of the biochar and modification methods for the enhancement of adsorption efficiency of the biochar, (iii) the factors affecting the adsorption of U and F^- such as pH, biochar dosage, U and F^- concentration, co-existing ions, and temperature, (iv) adsorption mechanisms, (v) adsorption isotherms, kinetics, and thermodynamics, and (vi) challenges and limitations for real U and F^- groundwater treatment. Lastly, this paper concludes with future studies and recommendations for in-depth research on removing U and F^- using low-cost biochars.

2. Methodology

To address the objectives, extensive research was performed from scholarly databases (Scopus, ScienceDirect, and Web of Science) on U and F⁻ removal using biochar. The following keywords and synonyms in different combinations: 'biochar', 'sorption', 'water treatment', 'uranium', 'fluoride removal', 'pollutant/contaminant removal', 'heavy metal removal', 'aqueous solution', 'groundwater', 'adsorption', 'modification', 'mechanism', 'biomass adsorbent', 'crop residue', 'agricultural biomass', 'reusability', and 'regeneration' were used for the literature search. More than 1100 studies were identified using these keywords from three different databases. Duplicates were removed using Endnote, and studies that reported metal removal other than the ones under investigation were not considered for this review. More than 300 papers were retrieved after excluding duplicates and studies that were irrelevant. Selected articles were further scrutinized based on the abstract, and approximately 89 studies focusing on U and F⁻ removal from aqueous solution/wastewater/groundwater were included in this review. The papers on biochar (studies of U and F⁻ removal) covered the period from 2011 to 2022. Publications were distributed in order, with 37 studies on F⁻ removal and 52 on U removal. Prisma flowchart was used for displaying data collection, exclusion and inclusion criteria (Figure 1).

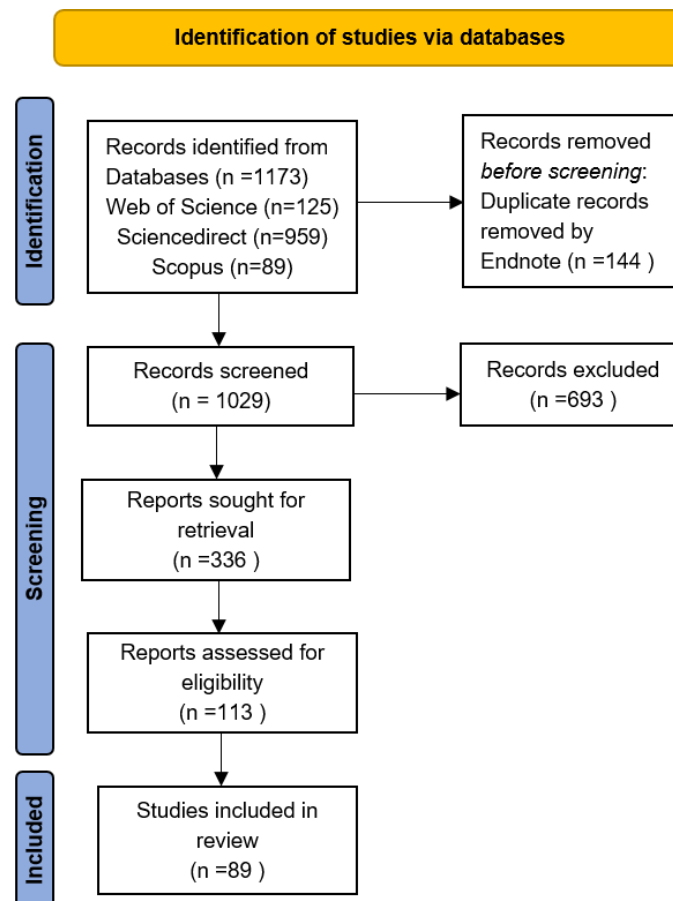


Figure 1. PRISMA flowchart showing data collection, exclusion, and inclusion criteria.

3. Results and Discussion

3.1. Role of Different Feedstock Types on Biochar Properties

Biochar has been obtained from pyrolyzing different feedstocks to remove U and F⁻, due to their inherent and excellent physiochemical properties. Generally, woody biomass and crop residues are comprised of cellulose, hemicellulose, and lignin. Feedstocks such as crop residues (sugarcane bagasse, rice husk, wheat straw, rice straw, etc.), grasses, and softwood (pine) are composed of a large proportion of cellulose and hemicellulose and

degrade faster due to lower thermal resistance [69,70]. As a result, cellulose and hemicellulose degrade at lower temperatures (200–400 °C), while lignin has a wide decomposition range (200–900 °C) [57,69,71]. Hence, softwood and crop residues require low temperatures for pyrolysis. Biochar yield is less in this case because biomass with high cellulose and hemicellulose contain aliphatic carbon phases, which can easily break. Thus, they do not make stable biochar and produce low biochar yield. These feedstocks produce high-oxygen-containing functional groups such as carboxyl, carbonyl, and hydroxyl [69,70,72,73].

On the other hand, hardwoods (eucalyptus) are composed of a high fraction of lignin; therefore, they require higher temperatures for degradation. These feedstocks make stable biochar because they contain aromatic monomers and high carbon content making them thermally stable and thus producing high biochar yield [69,70]. Some feedstocks which are not plant-based/non-woody, such as animal manure and sludge, also degrade faster. Thus, they require a low temperature range for biochar preparation [70,72,74]. Biochar prepared at high temperatures is suitable for the sorption of organic contaminants, while the sorption of inorganic contaminants requires low temperatures [45,70,75]. As a result, crop residues, grasses, and manure-based feedstocks are beneficial for U and F adsorption as they have oxygen-based functional groups [74,76].

3.2. Applications of Biochar in U and F⁻ Remediation

Biochar has gained much attention due to its widely available feedstock, making it a low-cost adsorbent, and it possesses high surface area, porosity, and oxygen-rich functional groups [77]. This section describes the application of biochar for removing U and F⁻ from the water and their efficiency.

U is a ubiquitous radioactive element, and its presence in water makes it unfit for drinking and causes many toxic effects on kidneys, bones, and the liver [8–10]. Various treatment technologies have been developed for U removal, such as reverse osmosis, ion exchange, coagulation, and adsorption [78,79]. Of these, adsorption by biochar is the most cost-effective method [72,80]. Several kinds of research have been performed on the bioremediation of U-contaminated water through biochar, described in this section.

Feedstocks, modification methods, and optimum operating conditions such as pyrolysis temperature, residence time, pH, and biochar dosage were employed to remediate U and F⁻ through biochar (Figure 2). For instance, rice husk biochar was employed for U removal, which showed a removal efficiency of 99.8% and adsorption capacity of 138.88 mg g⁻¹ (Table 1) at pH 5.5 and temperature range of 303–353 K with a biochar dose of 0.38 g L⁻¹ and initial U concentration of 3 mg L⁻¹ [81]. Jin et al. [82] examined wheat straw biochar which exhibited a maximum sorption capacity of 355.6 mg g⁻¹ at pH 4.5, temperature of 25 °C, with initial concentration of 10 mg L⁻¹. HNO₃-modified rice straw biochar significantly removed U with a sorption capacity of 242.65 mg g⁻¹ (oxidized biochar) and 162.54 mg g⁻¹ (raw biochar) at pH 5.5, a temperature of 25 °C, and dose of 0.01 g L⁻¹. HNO₃ oxidation increased the surface area, porosity, and oxygen-containing functional groups [33]. Pine-needles-based biochar successively removed U with a maximum adsorption capacity of 623.7 mg g⁻¹ at pH 6, a temperature of 25 °C, and dosage of 5 g L⁻¹ [37]. Dai et al. [34] reported U removal from corn-cob-based biochar with a sorption capacity of 163.18 mg g⁻¹ at pH 6, temperature of 25 °C, and biochar dose of 5 g L⁻¹. Palm-based biochar was investigated for U removal, which showed a removal efficiency of 99.2% and maximum sorption potential of 488.7 mg g⁻¹ at pH 3 and 25 °C [36]. Guo et al. [83] successfully removed U using sponge gourd biochar with a sorption capacity of 239.21 mg g⁻¹ at pH 5, temperature of 30 °C, and initial concentration of U given 5 mg L⁻¹. Similarly, Ioannou et al. [84] prepared sponge gourd biochar which exhibited an excellent U sorption potential of 904 mg g⁻¹ at pH 3 and 23 °C. Lingamdinne et al. [85] employed magnetically modified watermelon rind biochar which showed a U uptake of 323.56 mg g⁻¹ for modified biochar and 135.86 mg g⁻¹ for pristine biochar at pH 4 and 20 °C. The high sorption capacity was due to the magnetization of biochar by Fe oxide, resulting in increased surface area, porosity, and sorption potential.

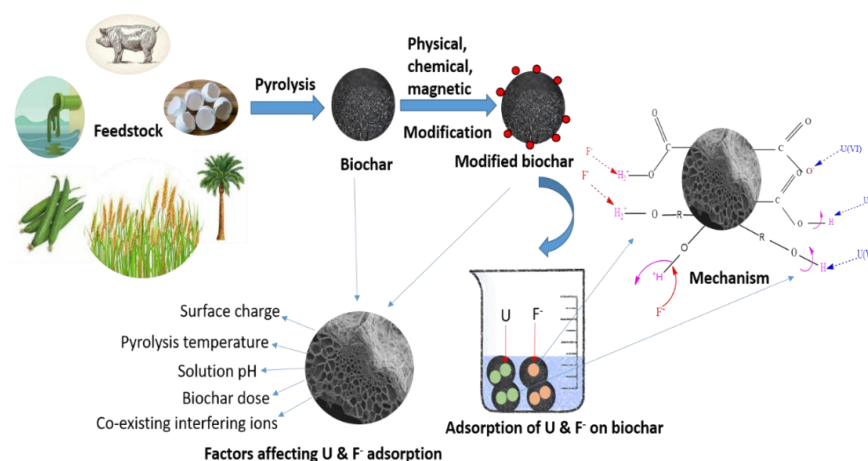


Figure 2. Schematic diagram of U and F[−] adsorption on biochar.

Drinking F[−]-contaminated water can cause serious health issues such as skeletal fluorosis, dental fluorosis, bone cancer, and brain damage [86–88]. Various research works have been conducted on F[−] removal using biochar, such as Zhou et al. [89] who prepared La/Fe/Al oxide-loaded rice straw biochar with a maximum F[−] sorption capacity of 10.85 mg g^{−1} for raw biochar while 111.11 mg g^{−1} for the modified one (Table 1), in the pH range of 3 to 11 with an initial F[−] concentration of 6 mg L^{−1}. Wheat-straw-derived biochar impregnated with Al(OH)₃ and La(OH)₃ was used for F[−] removal from water. The prepared biochar showed 98.69% removal with a maximum F[−] uptake of 51.28 mg g^{−1} at pH 7 and a temperature of 25 °C [90]. Nanoscale rice husk biochar was studied for defluoridation with a removal efficiency of 90% and maximum F[−] adsorption capacity of 17.3 mg g^{−1} at pH 7 and a temperature of 30 °C [24]. Mohan et al. [91] utilized magnetic corn stover biochar, which removed F[−] at pH 2, with a maximum sorption capacity of 4.11 mg g^{−1}. *Tamarix hispida*-based biochar showed 99.6% removal from synthetic water and 86.69% from real wastewater. The biochar exhibited an adsorption potential of 164.23 mg g^{−1} at pH 6 and temperature of 25 °C [40]. Coconut-derived biochar was used for defluoridation with a removal efficiency of 82.45% at pH 6.27 and a solution temperature of 30 °C [92]. Seed shells of *Camellia oleifera* (tea oil plant) were utilized for biochar production to remove F[−] from aqueous solution and exhibited an adsorption capacity of 11.04 mg g^{−1} at pH 6.8 [93]. Watermelon rind biochar easily removed F[−] at pH 1 with a maximum sorption capacity of 9.5 mg g^{−1} [94]. Wang et al. [95] prepared pomelo-peel-based biochar for defluoridation, which showed 100% removal efficiency with a sorption potential of 18.52 mg g^{−1} at pH 6.5. Okra stem biochar effectively removed F[−] with an adsorption capacity of 20 mg g^{−1} at pH 2, a temperature of 35 °C, and with an initial concentration of 10 mg L^{−1} [96]. A biochar composite of *platanus acerifoli* leaves and eggshell showed an excellent removal efficiency of 98.53% with a maximum adsorption capacity of 308 mg g^{−1} at pH 5 and 25 °C [97].

Discussed above are some of the studies about the application of biochar in U and F[−] remediation. It was observed that the adsorption capacity of biochar depends on various parameters such as feedstock, modification, pH, dose, temperature, initial concentration of U and F[−] in the solution, and functional groups. The effects of these parameters are discussed in Sections 3.5 and 3.7. Table 1 summarizes the various research works carried out on U and F[−] removal using biochar.

3.3. Synthesis of Biochar

The thermochemical conversion of biomass is the most common method for the production of biochar [98]. It includes pyrolysis, gasification, torrefaction, and hydrothermal carbonization [72]. For better biochar yield, parameters such as feedstock type, carbonization temperature, modification methods, heating rate, residence time, solution pH, adsorption temperature, adsorbent dosage, etc., must be optimum because of their significant

impact on the physicochemical properties of the biochar [74,99,100]. Different categories of feedstock have been utilized for the synthesis of biochar, such as crop residues (corn stover, rice straw, rice husk, wheat straw, corn cob, etc.) [73,101,102], woody biomass (pine needles, pine sawdust, bamboo, eucalyptus wood, palm tree fibres, etc.) [103–105], fruit waste (watermelon rind and orange peel) [94,106], animal waste (pig manure, horse manure, and dairy manure) [107–109], sewage sludge [110], etc. For example, Jin et al. [82] derived biochar from cow manure and wheat straw for U removal from water. It was found that cow-manure-derived biochar exhibited higher removal efficiency than wheat straw-derived biochar. Because of higher ash content, surface oxygen (which bonded with U ions) and Ca^{2+} occurred on the surface, exchanged with positively charged U ions, and provided new adsorption sites on the surface of cow-manure-derived biochar.

Furthermore, carbonization temperature is also an essential parameter for synthesis as it affects the pore volume and surface area of the biochar. For instance, Hu et al. [111] pyrolyzed bamboo sawdust at different temperatures (300, 450, and 600 °C). It was observed that surface area and pore volume were positively correlated with the pyrolysis temperature, i.e., the pore volume and surface area of the biochar were enhanced with increasing pyrolysis temperature, resulting in higher U uptake. However, Alkurdi et al. [112] pyrolyzed sheep bone to derive bone char for F^- removal at different temperatures (500, 650, 800, and 900 °C). The surface area of bone char decreased from 120.031 $\text{m}^2 \text{g}^{-1}$ to 89.06 $\text{m}^2 \text{g}^{-1}$; as a result, the pore volume decreased from 0.283 $\text{m}^3 \text{g}^{-1}$ to 0.235 $\text{m}^3 \text{g}^{-1}$, with increased pyrolyzing temperature from 500 °C to 900 °C due to pore shrinkage and pore breakage at very high temperatures.

Modification is another critical parameter in the synthesis of biochar, which is performed prior to or after the pyrolysis of raw biomass to improve the adsorption capacity, surface morphology, and physiochemical properties of the biochar. For instance, Lingamdinne et al. [85] magnetically modified watermelon rind biochar for U removal. They found that magnetization improved the surface morphology from poorly structured to a porous and ordered structure of the biochar and enhanced the surface area from 52.1 $\text{m}^2 \text{g}^{-1}$ to 86.35 $\text{m}^2 \text{g}^{-1}$. U uptake was enhanced from 135.86 mg g^{-1} to 323.56 mg g^{-1} after the magnetization. Different biochar modification methods are further discussed in Section 3.5. The various biochar production techniques are as follows:

3.3.1. Pyrolysis

The pyrolysis process commonly produces biochar, and this process involves the thermal degradation of biomass into solid (biochar), liquid (bio-oil), and gas (syngas) in oxygen-limited conditions at high temperatures ranging from 300 to 700 °C [113,114]. Pyrolysis is further classified into slow and fast pyrolysis based on the pyrolysis temperature, heating rate, and residence time. In slow pyrolysis, biochar is the primary product, while the major products in fast pyrolysis are bio-oil and syngas. Compared to fast pyrolysis, slow pyrolysis is better for biochar production because biochar yields decrease with an increase in temperature and heating rate [114,115].

3.3.2. Gasification

Gasification is the thermal decomposition of solid carbonaceous material derived from fossil fuels such as wood or coal into producer gas known as syngas at high temperature (>700 °C) with gasifying agents such as steam, oxygen, air, etc., to partially oxidize the feedstock [72,114,115]. During gasification, the major product is syngas, while biochar is produced as a by-product with a lower yield [72].

3.3.3. Torrefaction

Torrefaction is a pretreatment process before pyrolysis to improve the properties of the biomass. Torrefaction increases the hydrophobicity, further enhancing the biochar's storage stability, grindability, and carbon content. Reducing oxygen, water, or moisture from biomass increases the biochar yield [116]. Torrefaction is known as mild pyrolysis,

operating at low temperatures and heating rates. Biomass is pyrolyzed in the temperature range of 200–300 °C, at a heating rate of $<50\text{ °C min}^{-1}$, having a residence time of less than 30 min under anaerobic conditions and atmospheric pressure [116,117].

3.3.4. Hydrothermal Carbonization

Hydrothermal carbonization is used for making biochar from wet biomass. It helps improve the properties of the biomass, such as hydrophobicity, grindability, increased carbon content, and reduced oxygen content. It is specially employed for feedstock such as sewage sludge, animal and human wastes, compost, municipal wastes, etc. As biomass does not require drying before the treatment, it is better and more economical than pyrolysis and gasification [113,114].

3.4. Characteristics of Biochar

Scanning electron microscopy–electronic dispersive X-ray (SEM-EDX) analyses the biochar's surface morphology and elemental mapping. For example, Ahmed et al. [38] determined the surface morphology and elemental composition using SEM-EDS. They concluded the fibrous–porous structure of the biochar and the presence of C, O, Fe, Mn, and Na on the biochar surface, which confirmed the MnFe_2O_4 fabrication of the biochar. The surface area of biochar is analysed using the Brunauer–Emmett–Teller method (BET). For instance, Guilhen et al. [36] performed the BET method and found that the surface area of biochar increased from 0.8320 to 643.12 $\text{m}^2\text{ g}^{-1}$ after CO_2 activation, resulting in a high adsorption capacity of the biochar, which confirmed that physical activation has potential to enhance U uptake using biochar.

Fourier-transform infrared spectroscopy (FTIR) is used to observe the functional groups on biochar surfaces. For example, several previous studies have utilized acid-modified biochar and found that C–O, C=O, O–H, C–H, and –COOH were the main functional groups present on the biochar surface [7,33,35,82,111,118–121]. Biochars treated with a base showed C=O, N–H, C–H, C–O, O–H, and C–OH as the major functional groups [90,122–124]. Magnetized biochars showed different functional groups such as Fe–O, C=O, C–O, O–H, C=C, C–H, C–O–C, and Si–O–Si [39,85,91,125–127]. Ahmed et al. [38] and Hu et al. [105] observed that a new peak was detected at 909 cm^{-1} and 916 cm^{-1} , which corresponded to the stretching vibration of $[\text{U}=\text{O}=\text{U}]^{2+}$ and confirmed U adsorption on the biochar surface. Similarly, Sadhu et al. [94] observed a new adsorption peak at 997 cm^{-1} , which corresponded to C–F stretching and indicated F^- adsorption.

X-ray photoelectron spectroscopy (XPS) examines the elemental composition and chemical state of atoms in a produced material and provides information about the adsorption mechanism. For example, Ding et al. (2018) found that adsorbed U was a mixture of 87% U(IV) and 13% U(VI). X-ray diffraction (XRD) is used to analyse the crystallographic structures of prepared biochar and the dominant minerals present on the biochar surface. For instance, Wei et al. [128] performed XRD and found that the crystalline size of CeO_2 , which was dispersed onto the biochar surface, was 17.07 nm. Similarly, Halder et al. [92] observed several peaks which showed the presence of fluorinated compounds such as K_2MgF_4 and KFeF_3 and confirmed the F^- sorption onto the biochar surface.

3.5. Modification Methods

Modification is necessary to improve biochar properties such as surface area, pore structure, and functional groups [129]. Modification has four types: physical modification, chemical modification, magnetic modification, and impregnation or coating of the minerals [130]. Modification or activation can be conducted before or after pyrolysis. Figure 3 shows the different modification methods, including physical, chemical, and magnetic modification and Table 1 summarizes the effect of different modification methods on the properties of biochar for U and F^- removal.

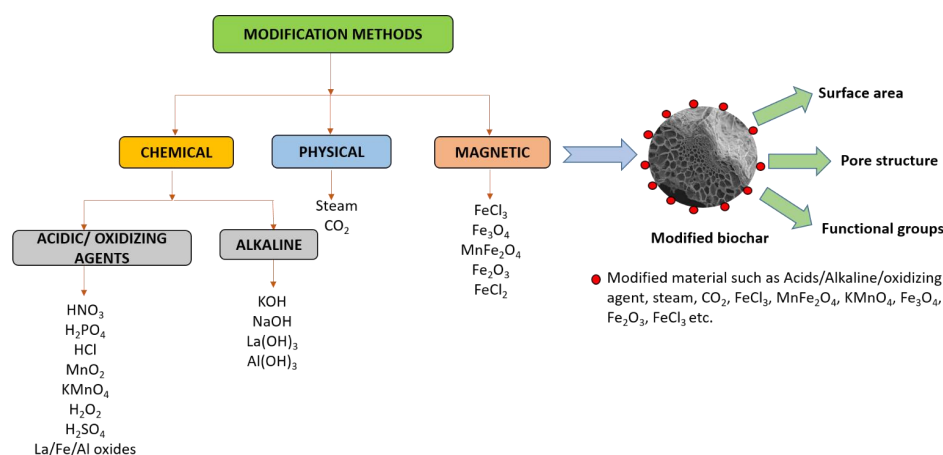


Figure 3. Schematic diagram representing different modification methods of biochar which affect the different properties of biochar, including surface area, pore structure, functional groups on biochar surface, etc.

3.5.1. Physical Modification

Physical modification involves the utilization of oxidizing agents such as CO_2 , air, steam, and ozone at high temperatures above $700\text{ }^\circ\text{C}$. It is generally employed for increasing the surface area and porosity of biochar [164]. For instance, Guilhen et al. [36] removed U from aqueous solution using biochar modified with CO_2 as an activation agent at the temperature range of $700\text{--}1000\text{ }^\circ\text{C}$. The CO_2 activation increased the aromaticity and porosity of the biochar with the increase in surface area from 0.83 to $643\text{ m}^2\text{ g}^{-1}$ and enhanced the removal efficiency from 80.5% (primary biochar) to 99.2% (activated biochar). Activation made the adsorption sites more heterogenous and as a result created more pores of biochar. Similarly, Halder et al. [92] employed the steam activation of biochar at $900\text{ }^\circ\text{C}$ for F^- removal from aqueous solution, resulting in enhanced porosity and a surface area of $1054\text{ m}^2\text{ g}^{-1}$. Steam activation of the biochar resulted in an increased removal efficiency of 82.45% . Steam activation created more adsorption sites by releasing volatile compounds during the activation process.

3.5.2. Chemical Modification

Chemical modification is carried out via acids, oxidizing agents, and alkaline treatment. Acid modification enhances the surface area, improves surface morphology, pore structure, and enriches the biochar surface with oxygen-containing functional groups such as carboxylic (COO^-), hydroxyl (OH^-), carbonyl (CO), etc., resulting in a negative surface charge of the biochar and promoting enhanced adsorption of the cationic species [120,130]. For example, HNO_3 modification induced negative charge on the biochar surface due to oxygen-containing functional groups and enhanced the U removal through complexation between positive U species and acidic functional groups. This modification provided high surface area, porosity, and microporous and mesoporous structure, resulting in higher stability and performance over pristine biochar (Table 1) [33,82,118–121]. Similarly, Guan et al. [35] modified pine tree sawdust biochar with the phosphoric acid–microwave method for F^- removal. The fabricated biochar showed an increase in surface area from 7.7 to $389.95\text{ m}^2\text{ g}^{-1}$, a decrease in pore diameter from 17 to 0.9 \AA , and an enhanced adsorption capacity of 0.885 mg g^{-1} . The modification removed some impurities from the pores of pristine biochar resulting in the availability of more active sites for F^- adsorption. The acid treatment protonated the surface functional groups such as hydroxyl and carboxyl, resulting in electrostatic attraction between F^- and protonated functional groups. De et al. [7] modified biochar with hydrochloric acid for F^- removal. This modified biochar showed increased active sites, a graphite-like carbon structure, and high carbon content resulting in higher adsorption than the raw biochar with a removal efficiency of 98.5% and adsorption potential of 1.11 mg g^{-1} .

Table 1. Effect of modification on the adsorption capacity of biochar for U and F[−] removal.

Feedstock	Modification	Target Contaminant	Surface Area (m ² g ^{−1})	Pore Structure	Adsorption Capacity (mg g ^{−1})/Removal Efficiency (%)		References
					Raw Biochar	Modified Biochar	
Rice straw	Hydroxyapatite–biochar nanocomposite	U	157.96	Mesoporous	110.56	428.25	[131]
Rice straw	HNO ₃ oxidation	U	-	Mesoporous	162.54	242.65	[33]
Wheat straw	HNO ₃ oxidation	U	290.1	-	8.7	355.6	[82]
Rice husk	Magnetization by Siderite	U	109.65	Mesoporous	-	52.63	[125]
Rice husk	Silicon containing biochar-supported iron oxide nanoparticles	U	62.88	-	-	138.88	[81]
Rice husk	Magnetic modification using Fe ²⁺ /Fe ³⁺ plus SO ₄ ^{2−} solution	U	109	-	64	118	[132]
Corn cob	Thermal air treatment at 300 °C	U	-	Mesoporous	68.82	163.18	[34]
Pine needles	Magnetization of oxidised biochar (HNO ₃ treated) by FeCl ₃	U	-	-	-	623.7	[37]
Pine sawdust	MgO/biochar composite	U	51.45	Mesoporous	-	514.72	[133]
Macaúba palm	CO ₂ activation	U	643.12	Microporous	-	488.7	[36]
Palm tree fibres	HNO ₃ oxidation	U	-	-	-	112	[121]
Bamboo sawdust	Phytic acid	U	1298	-	16.2	229.2	[111]
Bamboo biomass	Phosphate impregnation biochar cross-linked Mg–Al layered double-hydroxide composite	U	445.17	Microporous	15.869	274.15	[134]
Cactus fibre	HNO ₃ oxidation	U	<5	Microporous	-	214	[118]
Chinese banyan aerial root	KMnO ₄ modification	U	284	Mesoporous	19.08	27.29	[135]
Puncture vine	Magnetization by FeCl ₃	U	-	Mesoporous	-	17.24	[39]
Hydrophyte biomass	Magnetization by FeCl ₂	U	92.43	-	52.36	54.35	[136]
Hydrophyte	Phytic acid modification	U	433	-	-	128.5	[137]
Pig manure	KMnO ₄	U	-	-	369.9	979.3	[107]
Pig manure	H ₂ O ₂	U	-	-	369.9	661.7	[107]
Pig manure	NaOH	U	227.9	Mesoporous	369.9	952.5	[138]
Pig manure	HCl	U	36.3	Mesoporous	369.9	53.3	[138]
Pig manure	NaOH	U	345.7	Microporous	45.8	221.4	[124]
Pig manure	H ₂ O ₂	U	189	Microporous	45.8	145.1	[124]
Horse manure	Bismuth impregnation	U	-	-	186	516.5	[108]
Horse manure	MgCl ₂ modification	U	-	-	-	625.8	[139]
Cow manure	HNO ₃ oxidation	U	101.5	-	64	73.3	[82]
Carp fish scales	KOH activation	U	1074.73	Microporous	71.59	291.98	[122]
Sewage sludge	Thermal air treatment	U	-	Mesoporous	78.66	96.73	[34]
Sewage sludge	Air roasting–oxidation	U	623.09	Mesoporous	139.5	490.2	[140]
Winery waste (grape peels)	Chemically modification by NaOH, Na ₂ CO ₃	U	-	-	-	255	[141]
Winery waste (grape peels)	Thermal modification at 650 °C and oxidized with HNO ₃	U	165	-	-	100	[141]
Malt spent rootlets	HNO ₃ oxidation	U	540	Mesoporous	547	500	[120]
Coffee espresso residue	HNO ₃ oxidation	U	700	Mesoporous	547	357	[120]
Olive kernels	HNO ₃ oxidation	U	510	Mesoporous	357	381	[120]
Fungi	Sulfide nano zero valent iron	U	102.7	-	-	427.9	[142]
Green algae	Mn impregnation	U	63.7	Mesoporous	-	100.2	[143]
Cyanobacteria	Magnetic modification using Fe ₃ O ₄	U	-	-	58.05	52.06	[144]
Sponge gourd	ZnO-modified biochar hydrogel	U	-	-	-	239.21	[83]
Sponge gourd fibres	MnO ₂ oxidation	U	<5	Microporous	95	904	[84]
Sponge gourd sponges	HNO ₃ oxidation	U	-	-	-	92	[119]
Sponge gourd sponge	Salophen modification	U	-	-	-	833	[145]
Sponge gourd residue	Functionalization by hummer method	U	-	-	-	382	[146]
Watermelon rind	Magnetization by co-precipitation	U	86.35	-	135.86	323.56	[85]

Table 1. Cont.

Feedstock	Modification	Target Contaminant	Surface Area (m ² g ⁻¹)	Pore Structure	Adsorption Capacity (mg g ⁻¹)/Removal Efficiency (%)		References
					Raw Biochar	Modified Biochar	
Watermelon seeds	MnFe ₂ O ₄ modification	U	-	Mesoporous	21.24	27.61	[38]
Longan shell (fruit)	Nano zero valent iron	U	1168.88	Mesoporous	-	331.13	[77]
Orange peel	MnO ₂ modification	U	273.25	Mesoporous	165.4	246.3	[106]
Orange peel	Hydrogel	U	-	-	-	263.2	[147]
Tea waste	Iron manganese oxide	U	12	-	-	510.8	[148]
Rice straw	La/Fe/Al oxides impregnation	F ⁻	95.36	Mesoporous	10.85	111.11	[89]
Wheat straw	Impregnation of aluminium and lanthanum hydroxide	F ⁻	-	-	-	51.28	[90]
Rice husk	Chemical modification by iron	F ⁻	58.98	Mesoporous	-	4.45	[149]
Rice husk	Nano-scale size reduction	F ⁻	-	-	-	17.3	[24]
Rice husk	Magnetic biochar anchored with Al and Mg	F ⁻	114	Mesoporous	-	21.59	[150]
Corn stover	Magnetization by Fe ³⁺ /Fe ²⁺ solution	F ⁻	3.61	Microporous	6.42	4.11	[91]
Chir pine	Calcium pretreated	F ⁻	-	-	-	16.72	[151]
Mongolian scotch pine tree sawdust	Phosphoric acid-microwave method	F ⁻	339	Microporous	-	0.885	[35]
Douglas fir (pine)	Magnetization by Fe ₂ O ₃ /Fe ₃ O ₄	F ⁻	494	Microporous	-	9.04	[152]
Douglas fir (pine)	Iron-titanium biochar composite	F ⁻	576	Microporous	-	36	[153]
Reed biomass	Ce-loaded biochar beads	F ⁻	236.84	Mesoporous	-	34.86	[128]
Kashgar tamarisk	Lanthanum chloride	F ⁻	164.52	Mesoporous	-	164.23	[40]
Tea oil plant (seed shells)	Impregnation of zirconium dioxide	F ⁻	-	-	-	11.04	[93]
Sawdust	Chemical modification via cross-linking and protonation of the chitosan-sawdust biochar beads	F ⁻	57.97	Microporous	-	4.413	[154]
Pongamia pinnata seed cake	Engineered biochar by HCl solution	F ⁻	10.1	Microporous	-	1.11	[7]
Coconut	Steam activation	F ⁻	1054	Mixture of micropores and mesopores	-	82.45%	[92]
Pomelo peel	Impregnation of polypyrrole	F ⁻	-	-	-	18.52	[95]
Peanut shell	MgO	F ⁻	182.3	Mesoporous	-	83.05	[155]
Spent mushroom compost	Al(OH) ₃ coating	F ⁻	28.5	-	-	36.5	[13]
Food waste	AlCl ₃ impregnation	F ⁻	20.95	-	-	123.4	[156]
Tea waste	Chemical modification by H ₂ SO ₄ , NaNO ₃ , KMnO ₄	F ⁻	11.833	Macroporous	-	52.5	[157]
Red algae seaweed	Spent biochar	F ⁻	319.47	Microporous	-	2.1	[158]
Dairy manure	Calcium modification	F ⁻	2.6	-	0.11	0.42	[109]
Tea waste	Magnetic modification	F ⁻	115.65	Mesoporous	-	18.78	[159]
Peanut hull	Nil	F ⁻	98.2	Mesoporous	3.665	-	[160]
Pinecone	AlCl ₃	F ⁻	-	-	-	14.07	[161]
<i>Conocarpus erectus</i>	Nil	F ⁻	9.88	Microporous	205.7	-	[162]
Yak dung	FeCl ₂	F ⁻	-	-	-	3.928	[163]

U: Uranium; F⁻: Fluoride; -: data not available.

Oxidizing agents such as manganese oxide (MnO_2) [84,106], hydrogen peroxide (H_2O_2) [107,124], and potassium permanganate (KMnO_4) [107,135] were used to modify biochar for U removal, while metal oxides, such as iron oxide, aluminium oxide, and lanthanum oxide [89], were used to modify the biochar surface for F^- adsorption. These oxidizing agents showed enhanced adsorption due to a rise in surface area, porosity, and oxygenated functional groups on the biochar surface [165].

Alkaline treatment was given by metal hydroxides, such as KOH [122], NaOH [124,138], $\text{La}(\text{OH})_3$ [90], and $\text{Al}(\text{OH})_3$ [13]. For example, Saikia et al. [123] reported that the removal efficiency of F^- by perennial-grass-based biochar activated by adding KOH pellets was 24.8%. After activation, they observed a rise in surface area from $5.57 \text{ m}^2 \text{ g}^{-1}$ to $1248.2 \text{ m}^2 \text{ g}^{-1}$. Similarly, Chen et al. [13] observed an increased adsorption capacity of 36.5 mg g^{-1} and surface area from 3.6 to $28.5 \text{ m}^2 \text{ g}^{-1}$, and Yan et al. [90] reported increased F^- removal efficiency from 77.97% to 98.69% resulting from biochar modification with aluminium and lanthanum hydroxides. An increase in surface area was found because the coating of $\text{Al}(\text{OH})_3$ on the biochar surface was amorphous (the presence of small particles). Amorphous materials have more active sites for sorption [166].

3.5.3. Magnetic Modification

The magnetization of biochar increases the adsorption capacity by enhancing the surface area, pore volume, surface morphology, functional groups, and stability of the biochar. In addition, magnetic biochar can be reused multiple times through the separation of contaminants from biochar using an external magnetic field [61,85]. For instance, Ahmed et al. [39] produced biochar from *Tribulus terrestris* (puncture vine) and magnetized it using FeCl_3 to remove U(VI) from wastewater. The magnetic biochar exhibited a layered porous structure, which provided increased surface area and enhanced adsorption capacity. After the modification, there was an increase in oxygen content resulting in oxygen-containing functional groups. FTIR analysis revealed the presence of Fe–O, C=O, C–O, and –OH functional groups after the magnetization of biochar. Another study was carried out by Philippou et al. [37] for removing U from aqueous solution through magnetic modification using Fe_3O_4 -loaded pine needles biochar, which enhanced the adsorption capacity to 623.7 mg g^{-1} . Ahmed et al. [38] synthesized biochar from *Citrullus lanatus* L. (watermelon) seeds and used MnFe_2O_4 to magnetically modify biochar through the co-precipitation method for U(VI) removal from wastewater. It was observed that magnetic biochar exhibited a mesoporous structure, higher stability, enhanced adsorption capacity of 27.61 mg g^{-1} from 21.24 mg g^{-1} (pristine biochar), oxygenated functional groups, and increased availability of active sites on the biochar.

The impregnation of mineral salt solution increases the oxygen functional groups on the biochar surface, increasing the sorption capacity of the adsorbent. For instance, Zhou et al. [89] derived biochar from rice straw impregnated with La/Fe/Al oxides through co-precipitation for F^- removal from drinking water. Impregnation increased the production of hydroxyl groups on the biochar surface. Impregnated biochar enhanced the surface area from $2.59 \text{ m}^2 \text{ g}^{-1}$ to $95.36 \text{ m}^2 \text{ g}^{-1}$ and the adsorption capacity from 10.85 mg g^{-1} to 111.11 mg g^{-1} in a wide pH range of 3–11.

3.5.4. Thermal Air Treatment (TAT)

Dai et al. [34] applied the TAT method to modify the biochar to remove U(VI) from the aqueous solution. In this method, the biochar surface was engineered by heating biochar at $300 \text{ }^\circ\text{C}$ for 30 min to enhance the adsorption performance of the biochar. The adsorption capacity of the biochar increased from 68.82 mg g^{-1} to 163.18 mg g^{-1} . The resultant biochar exhibited a high O/C ratio resulting in oxygen-containing functional groups, a reduction in the average pore diameter (11.53 nm to 3.62 nm), and increased surface area (360.35 to $362.26 \text{ m}^2 \text{ g}^{-1}$), resulting in the development of a mesoporous structure, which facilitated U(VI) removal from the water. Compared to physical and chemical modification, thermal air

treatment (TAT) exhibited a lower carbonization temperature and shorter processing time resulting in elevated product yield and lower production cost and energy consumption.

3.6. Raw vs. Modified Biochar

Biochar (raw as well as modified) has been widely utilized for U and F⁻ removal from aqueous solution at several operating parameters such as pH, dose, temperature, initial concentration, etc. The following section discusses the comparative analysis of adsorption capacities with respect to raw and modified biochar at different experimental conditions. For example, Hu et al. [111] employed phytic-acid-modified bamboo sawdust biochar pyrolyzed at 450 °C to remediate U(VI) from synthetic water. The modified biochar showed a higher sorption capacity (229.2 mg g⁻¹) than raw biochar (16.2 mg g⁻¹) (Table 1) at pH 4 and 25 °C. Fabrication enhanced the surface area of the biochar from 8.47 m² g⁻¹ to 157.96 m² g⁻¹, nearly nineteen times higher than the pristine biochar. Modification enlarged the pores due to the release of volatile matter during pyrolysis, resulting in enhanced pore volume from 0.015 cm³ g⁻¹ (raw biochar) to 0.919 cm³ g⁻¹ (modified biochar). Phytic acid fabrication introduced phosphate-functionalized groups on the biochar surface and improved the pore structure, which enhanced the U(VI) uptake compared with raw biochar. Similarly, Ahmed et al. [33] used HNO₃-modified rice straw biochar to remove U(VI) from aqueous solution. Oxidized biochar exhibited an adsorption capacity of 242.65 mg g⁻¹, while raw biochar showed a maximum sorption capacity of 162.54 mg g⁻¹ at pH 5.5 and a temperature of 25 °C. Nitric acid enriched the carbonized surface with acidic functional groups such as carboxyl and carbonyl, thereby enhancing the adsorption ability of the biochar. Similar findings were reported by [82,118–121]. A novel adsorbent, hydroxyapatite biochar nanocomposite made from rice straw, was developed by Ahmed et al. [131] to remove U(VI) from laboratory water. The fabricated biochar exhibited an adsorption potential of 428.25 mg g⁻¹, while raw biochar showed an adsorption capacity of 110.56 mg g⁻¹. Essentially, hydroxyapatite is a calcium phosphate material which has a high tendency to remediate environmental contaminants [167]. Hence, introducing this biomaterial on the biochar surface enhanced its adsorption potential compared to raw biochar. The highest U(VI) uptake was observed at pH 5.5, a temperature of 25 °C, and initial concentration of 50 mg L⁻¹ in both the adsorbents. Modified biochar showed excellent removal efficiency >90% even after five sorption–desorption cycles. Han et al. [124] examined NaOH-modified pig manure biochar for U immobilization and observed that modified biochar exhibited more significant sorption potential (221.4 mg g⁻¹) than the pristine one (45.8 mg g⁻¹). The greater U uptake was due to the enhanced surface area (from 135.7 m² g⁻¹ to 345.7 m² g⁻¹), pore volume (0.032 cm³ g⁻¹ to 0.119 cm³ g⁻¹), and carboxyl and hydroxyl functional group complexation with U. A similar study was performed using alkali (NaOH)-modified pig manure biochar for U removal which supported these results [107].

Zhou et al. [89] employed tri-metallic (La/Fe/Al oxides)-modified biochar derived from rice straw for the defluoridation of aqueous solution. The modified biochar exhibited a maximum adsorption potential of 111.11 mg g⁻¹, while pristine biochar showed 10.85 mg g⁻¹ F⁻ uptake. The impregnation of metal oxides on the biochar surface enhanced the surface area (2.59 to 95.36 m² g⁻¹), pore volume (0.012 to 0.611 cm³ g⁻¹), and pore diameter (12.01 to 12.49 nm). As La/Fe/Al oxides have a positive charge and fluoride has negative, the fabricated biochar showed a higher capacity for F⁻ removal through ion exchange and electrostatic interactions. Generally, biochars are negatively charged [168]; hence, the raw biochar exhibited less F⁻ uptake than the modified biochar. Maximum removal was observed at pH 3, with a biochar dosage of 1 g L⁻¹, with an initial concentration of 6 mg L⁻¹ in both sorbents. Limited studies have compared raw and modified biochar in the case of F⁻. They have determined the adsorption capacities of only modified/coated/fabricated biochars.

Based on the available literature, it was observed that less acidic or near-neutral pH (discussed in Section 3.7.1), low-to-medium (200–550 °C) pyrolyzing temperature, a

solution temperature of 25 °C, and chemical (acidic) and magnetic modification of the biochar yielded better results for U adsorption. In the case of F⁻, alkali pH (see Section 3.7.1), a medium pyrolyzing temperature (450–700 °C), and a solution temperature of 30 °C, metal oxides and hydroxides, magnetization, and chemical (weak acids and alkali) modification might be more favourable for F⁻ removal.

3.7. Factors Affecting the Adsorption of U and F⁻ in Aqueous Solution

3.7.1. Influence of pH

Among various factors, the pH of the solution is one of the crucial factors which affects the adsorption of contaminants by governing their speciation and surface charge of biochar in varying-pH solution [84,107]. Speciation of U was influenced at varying pH; at pH values less than 6, U (VI) occurred in the form of uranyl species (UO₂²⁺) and positively charged hydroxy complexes, such as (UO₂)₃(OH)₄²⁺, (UO₂)₂(OH)₂²⁺, (UO₂)₃(OH)₅⁺, UO₂(OH)⁺, (UO₂)₄(OH)₇⁺, (UO₂)₃(OH)₅²⁺, and (UO₂)₂OH³⁺, and negatively charged species of U, i.e., (UO₂)₂CO₃ (OH)₃⁻ occurred at pH > 6 (Table 2) [169,170]. It was found that at lower pH values (3–6) (less acidic or near neutral), the biochar surface was negatively charged due to the presence of negatively charged functional groups (COO⁻, OH⁻) [171] and positively charged U species were present at these pH values [169]. In addition, when the solution pH > pHzpc, the surface charge on the biochar became negative, which attracted the positive U species through electrostatic attraction and complexation, resulting in a high adsorption capacity [133] (Table 2). Figure 4 summarizes how major parameters affect U and F⁻ adsorption.

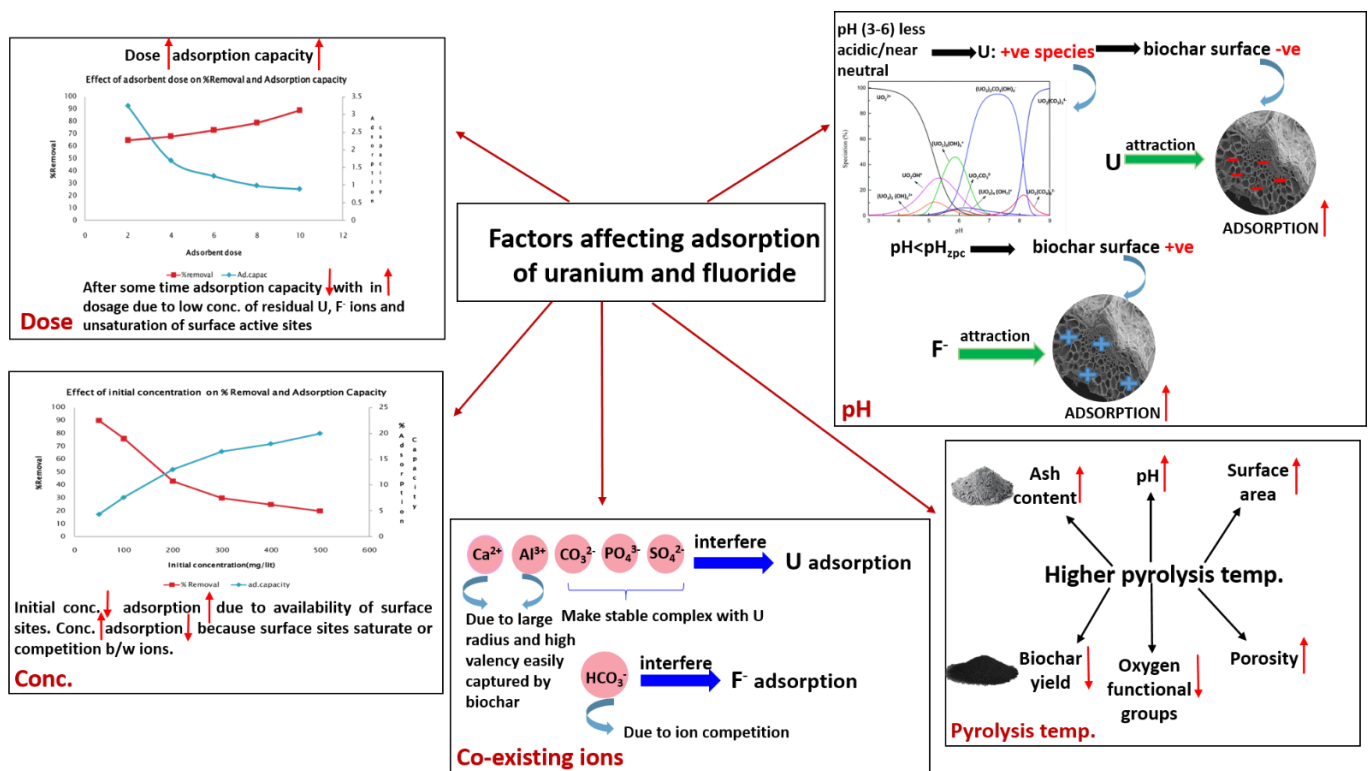


Figure 4. Effect of different parameters on the adsorption capacity and removal efficiency of U and F⁻, including biochar dose, initial concentration of U and F⁻, solution pH, pyrolysis temperature, and Co-existing ions.

For example, Ahmed et al. [39] have found that the adsorption of U (VI) increases with a rise in pH up to pH 6 and decreases at pH > 6 using magnetic-modified biochar. This occurred due to repulsion between negatively charged U species and the negatively

charged biochar surface at $\text{pH} > 6$. Hu et al. [105] examined the impact of pH on the adsorption capacity of U (VI) using bamboo shoot shell biochar at a pH ranging from 1 to 7 and found the maximum adsorption at pH 4 which decreased further with the increase in pH. This is because at $\text{pH} < 4$, electrostatic repulsion occurred between the positively charged biochar surface (due to protonation of functional groups—carboxyl and hydroxyl groups) and positively charged U species; hence, adsorption is less. Biochar was positively charged when the pH was highly acidic (1–2) due to the protonation of functional groups leading to repulsion between positive U species and the positive biochar surface. It was observed that slightly acidic or near-neutral pH favoured high adsorption capacities for U because of the presence of negatively charged functional groups due to the deprotonation of functional groups and smaller pH_{PZC} values, which led to attraction between positive U species and the negative biochar surface, whereas at basic pH values, the biochar was negatively charged due to the deprotonation of functional groups resulting in repulsion between negative species of U and the negative biochar surface.

The interaction between biochar and F^- is affected by the point of zero charge (pZC). As the solution pH is less than pH_{PZC} , it favours the adsorption of F^- electrostatically [89]. Table 3 shows the influence of the solution pH on the biochar adsorption capacity for F^- removal. For instance, Habibi et al. [40] synthesized lanthanum-chloride-activated biochar, which had a pH_{PZC} of 6.6, and reported that F^- removal increased at $\text{pH} < 6.6$ and gradually decreased at $\text{pH} > 6.6$. At varying pH, the protonation or deprotonation of functional groups on the biochar surface occurs. At low pH, the removal of anionic F^- species is favoured, as the functional groups present on the surface of the biochar are protonated [7]. At high pH, the removal of cationic species is favoured due to the deprotonation of functional groups present on the biochar surface. Sadhu et al. [94] observed a significant impact on the adsorption of F^- using watermelon rind biochar, which showed a maximum adsorption of F^- at pH 1, which was found to be 9.5 mg g^{-1} . Furthermore, a sharp decline in adsorption efficiency was observed above pH 2. Another reason for the high adsorption capacity was the electrostatic attraction between the positively charged biochar and F^- ions (Table 3). However, there are studies where F^- adsorption has occurred at higher pH values ($\text{pH} > 4$). This is due to ion exchange between F^- ions and the negatively charged or less positively charged biochar surface [90].

3.7.2. Effect of Biochar Dose on U and F^- Adsorption

For the optimum remediation of U and F^- , it is required to optimize the biochar dose by keeping the pH and the initial concentration of U and F^- constant. With increased biochar dosage, the adsorption capacity and removal percentage of U and F^- rose to the optimum level as the high dosage of the biochar provided many effective active sites on the biochar surface [107]. Table 4 shows the influence of biochar dosage on the adsorption capacity. For example, Yan et al. [90] observed that the F^- removal rate increased from 77.97% to 98.69% as the biochar dosage rose from 0.25 to 1 g L^{-1} . Xu et al. [176] identified that the U (VI) removal rate increased from 31.38 to 96.03% with the rise in biochar dose from 0.03 to 0.3 g L^{-1} . At the same time, a further increase in adsorbent doses decreased the adsorption capacity.

3.7.3. Influence of Initial Concentration

The initial concentration of U and F^- in aqueous solution influences the adsorption capacity of biochar. The impact of initial F^- and U concentration on biochar adsorption capacity is shown in Table 5. With low initial concentrations of U, F^- , and fixed biochar dose, the adsorption of U and F^- ions increased due to the availability of active surface sites. Furthermore, as the initial concentration of U and F^- increased, the adsorption decreased because fewer surface active sites were available, and there was more competition between the ions [13,105,118]. For instance, Goswami and Kumar [24] analysed that the removal rate of F^- declined from 90% to 68.3% with an initial F^- concentration increment from 3 to 10 mg L^{-1} , utilizing nanoscale rice husk biochar.

Table 2. Influence of solution pH on the adsorption of U.

Feedstock	Solution pH	pH _{PZC}	Target Pollutant	Speciation Adsorbed	Biochar Surface Charge	Adsorption Capacity (mg g ⁻¹)	References
Rice straw	5.5	2.5	U	UO ₂ ²⁺ , (UO ₂) ₃ (OH) ₅ ⁺ , (UO ₂) ₃ (OH) ₄ ²⁺ , (UO ₂) ₂ (OH) ₂ ²⁺	negative	428.25	[131]
Rice straw	5.5	2.5	U		negative	242.65	[33]
Wheat straw	6	3	U	UO ₂ ²⁺ , (UO ₂) ₃ (OH) ₅ ⁺ , (UO ₂) ₂ (OH) ₂ ²⁺ , UO ₂ OH ⁺ , (UO ₂) ₄ (OH) ₇ ⁺	negative	355.6	[82]
Rice husk	4	3.51	U	UO ₂ ²⁺ , UO ₂ OH ⁺ , (UO ₂) ₃ (OH) ₅ ⁺	negative	52.63	[125]
Rice husk	5.5	4.17	U	UO ₂ ²⁺ , (UO ₂) ₃ (OH) ₅ ⁺ , (UO ₂) ₂ (OH) ₂ ²⁺	negative	138.88	[81]
Rice husk	7	3.71	U	UO ₂ (OH) ⁺ , (UO ₂) ₂ (OH) ₂ ²⁺ , (UO ₂) ₃ (OH) ₅ ²⁺	negative	118	[132]
Corn cob	6	–	U	(UO ₂) ₃ (OH) ₅ ⁺ , (UO ₂) ₂ (OH) ₂ ²⁺ , UO ₂ OH ⁺	negative	163.18	[34]
Pine needles	6	3.8	U	–	–	623.7	[37]
Pine needles	6	–	U	–	–	62.7	[172]
Pine sawdust	4	2.98	U	UO ₂ ²⁺ , (UO ₂) ₃ (OH) ₅ ⁺ , (UO ₂) ₂ (OH) ₂ ²⁺ , (UO ₂) ₄ (OH) ₇ ⁺	negative	514.72	[133]
Macaúba palm	3	–	U	–	–	488.7	[36]
Palm tree fibres	6	–	U	–	–	112	[121]
Bamboo sawdust	4	2.73	U	UO ₂ ²⁺ , (UO ₂) ₃ (OH) ₅ ⁺ , (UO ₂) ₂ (OH) ₂ ²⁺ , UO ₂ OH ⁺	negative	229.2	[111]
Bamboo biomass	4	4.28	U	UO ₂ ²⁺ , (UO ₂) ₃ (OH) ₅ ⁺ , (UO ₂) ₂ (OH) ₂ ²⁺ , UO ₂ OH ⁺	–	274.15	[134]
Bamboo	6	–	U	–	–	–	[34]
Bamboo shoot shell	4	–	U	UO ₂ ²⁺ , (UO ₂) ₂ (OH) ₂ ²⁺ , UO ₂ OH ⁺ , (UO ₂) ₄ (OH) ₇ ⁺	negative	32.3	[105]
Cactus fibre	3	–	U	–	–	214	[118]
Camphor tree leaves	6.5	5.76	U	UO ₂ ²⁺ , (UO ₂) ₂ (OH) ₂ ²⁺ , UO ₂ OH ⁺	negative	98.29	[173]
Miswak branches	4	2.79	U	UO ₂ ²⁺ , (UO ₂) ₂ (OH) ₂ ²⁺ , UO ₂ OH ⁺	negative	85.71	[174]
Chinese banyan aerial root	4	–	U	–	–	27.29	[135]
Eucalyptus wood	5.5	–	U	(UO ₂) ₂ OH ³⁺ , (UO ₂) ₃ (OH) ₅ ⁺ , (UO ₂) ₂ (OH) ₂ ²⁺ , UO ₂ OH ⁺ , (UO ₂) ₄ (OH) ₇ ⁺	negative	27.2	[175]
Puncture vine	6	4	U	UO ₂ ²⁺ , (UO ₂) ₃ (OH) ₅ ⁺ , (UO ₂) ₃ (OH) ₄ ²⁺ , (UO ₂) ₂ (OH) ₂ ²⁺	negative	17.24	[39]
Water hyacinth	6	–	U	UO ₂ ²⁺ , (UO ₂) ₂ (OH) ₂ ²⁺ , UO ₂ OH ⁺ , (UO ₂) ₄ (OH) ₇ ⁺	negative	138.57	[176]
Hydrophyte biomass	3	4.2	U	UO ₂ ²⁺	–	54.35	[136]
Hydrophyte	4	2.46	U	UO ₂ ²⁺ , (UO ₂) ₃ (OH) ₄ ²⁺ , (UO ₂) ₂ (OH) ₂ ²⁺ , UO ₂ OH ⁺	negative	128.5	[137]
Switchgrass	5.9	–	U	UO ₂ ²⁺ , (UO ₂) ₃ (OH) ₅ ⁺ , (UO ₂) ₂ (OH) ₂ ²⁺ , UO ₂ OH ⁺	negative	4	[177]
Pig manure	4	–	U	–	–	979.3	[107]
Pig manure	4	–	U	–	–	661.7	[107]
Pig manure	4	–	U	–	–	952.5	[138]
Pig manure	4.5	–	U	UO ₂ ²⁺ , (UO ₂) ₂ (OH) ₂ ²⁺ , UO ₂ OH ⁺	–	221.4	[124]
Horse manure	4	9.05	U	UO ₂ ²⁺	–	516.5	[108]
Horse manure	4	–	U	UO ₂ ²⁺	negative	625.8	[139]
Cow manure	4.5	3	U	UO ₂ ²⁺ , (UO ₂) ₃ (OH) ₅ ⁺ , (UO ₂) ₂ (OH) ₂ ²⁺ , UO ₂ OH ⁺ , (UO ₂) ₄ (OH) ₇ ⁺	negative	73.3	[82]
Carp fish scales	5	2.87	U	UO ₂ ²⁺ , (UO ₂) ₃ (OH) ₅ ⁺ , (UO ₂) ₂ (OH) ₂ ²⁺ , UO ₂ OH ⁺	negative	291.98	[122]
Sewage sludge	6	–	U	(UO ₂) ₃ (OH) ₅ ⁺ , (UO ₂) ₂ (OH) ₂ ²⁺ , UO ₂ OH ⁺	negative	96.73	[34]
Sewage sludge	6	3	U	UO ₂ ²⁺ , (UO ₂) ₃ (OH) ₅ ⁺ , (UO ₂) ₂ (OH) ₂ ²⁺ , UO ₂ OH ⁺	negative	490.2	[140]
Winery waste (grape peels)	4	–	U	UO ₂ ²⁺	negative	255	[141]
Winery waste (grape peels)	4	–	U	UO ₂ ²⁺	negative	100	[141]
Malt spent rootlets (MSR)	3	–	U	–	–	547	[120]
Coffee espresso residue	3	–	U	–	–	547	[120]
Olive kernels	3	–	U	–	–	357	[120]
Fungi	5	6.41	U	–	positive	427.9	[142]
Green algae	6	2.62	U	(UO ₂) ₃ (OH) ₅ ⁺ , (UO ₂) ₂ (OH) ₂ ²⁺ , (UO ₂) ₄ (OH) ₇ ⁺	negative	100.2	[143]
Cyanobacteria	6	3.5	U	(UO ₂) ₃ (OH) ₅ ⁺ , (UO ₂) ₂ (OH) ₂ ²⁺ , UO ₂ OH ⁺	negative	58.05	[144]
Sponge gourd	5	–	U	(UO ₂) ₃ (OH) ₅ ⁺ , (UO ₂) ₂ (OH) ₂ ²⁺ , UO ₂ OH ⁺	negative	239.21	[83]

Table 2. Cont.

Feedstock	Solution pH	pH _{PZC}	Target Pollutant	Speciation Adsorbed	Biochar Surface Charge	Adsorption Capacity (mg g ⁻¹)	References
Sponge gourd fibres	3		U			904	[84]
Sponge gourd sponges	3	–	U	–	–	92	[119]
Sponge gourd sponge	5.5	–	U	–	–	833	[145]
Sponge gourd residue	6	1.8	U	UO ₂ ²⁺ , (UO ₂) ₃ (OH) ₅ ⁺ , (UO ₂) ₂ (OH) ₂ ²⁺ , UO ₂ OH ⁺	negative	382	[146]
Watermelon rind	4	5.4	U	–	–	323.56	[85]
Watermelon seeds	4	2.5	U	–	–	27.61	[38]
Longan shell (fruit)	6	6.25	U	–	–	331.13	[77]
Orange peel	5.5	2.6	U	UO ₂ ²⁺ , (UO ₂) ₃ (OH) ₄ ²⁺ , (UO ₂) ₂ (OH) ₂ ²⁺ , UO ₂ OH ⁺ , (UO ₂) ₂ OH ³⁺ , UO ₂ (OH) ₂	negative	246.3	[106]

U: Uranium; –: data not available; pH_{ZPC} = zero-point charge (pH value at which there is no charge).

Table 3. Effect of solution pH on biochar adsorption capacity for F⁻ removal.

Feedstock	Solution pH	pH _{ZPC}	Target Pollutant	Biochar Surface Charge	Adsorption Capacity (mg g ⁻¹)	References
Rice straw	8	11	F ⁻	positive	111.11	[89]
Wheat straw	7	4.8	F ⁻	negative	51.28	[90]
Rice husk	4	6	F ⁻	positive	4.45	[178]
Rice husk	7	–	F ⁻	–	17.3	[24]
Rice husk	5.3	–	F ⁻	–	21.59	[150]
Rice husk	6	–	F ⁻	–	1.856	[149]
Black gram straw	2	–	F ⁻	–	16	[96]
Corn stover	2	1.96	F ⁻	–	4.11	[91]
Chir pine	4.5	–	F ⁻	–	16.72	[151]
Mongolian scotch pine tree sawdust	7	–	F ⁻	–	0.885	[35]
Pine bark	2	9	F ⁻	positive	9.77	[179]
Pine wood	2	9	F ⁻	positive	7.66	[179]
Douglas fir	7	11	F ⁻	positive	9.04	[152]
Douglas fir	6	6.4	F ⁻	positive	36	[153]
Reed biomass	5.5	8.26	F ⁻	positive	34.86	[128]
Kashgar tamarisk	6	6.6	F ⁻	positive	164.23	[40]
Tea oil plant (seed shells)	6.8	4.45	F ⁻	negative	11.04	[93]
Sawdust	7	2.2	F ⁻	negative	4.413	[154]
Pongamia pinnata seed cake	7	–	F ⁻	–	1.11	[7]
Coconut	6.5	–	F ⁻	–	–	[92]
Cattail	–	–	F ⁻	–	1.28	[180]
Pomelo peel	6.5	8.6	F ⁻	positive	18.52	[95]
Watermelon rind	1	2.1	F ⁻	positive	9.5	[94]
Okra (lady finger) stem	2	–	F ⁻	–	20	[96]
spent Mushroom compost	10	–	F ⁻	–	4.7	[13]
Food waste	7.1	–	F ⁻	–	123.4	[158]
Tea waste	2	–	F ⁻	–	52.5	[109]
Red algae seaweed	5	6.9	F ⁻	positive	2.1	[169]
Dairy manure	5	8.8	F ⁻	positive	0.42	[109]
Sheep bone	–	–	F ⁻	–	2.33	[112]
Bone residues (chicken, cattle, and mixed bones)	–	–	F ⁻	–	4.29	[181]
Eggshell and platanus acerifoli leaves (5:1)	5	–	F ⁻	–	308	[97]

F⁻: Fluoride; -: data not available, pH_{ZPC}: zero-point charge (pH value at which there is no charge).

Table 4. Effect of biochar dosage on U and F⁻ adsorption.

Feedstock	Biochar Dose (g L ⁻¹)	Target Pollutant	Adsorption Capacity (mg g ⁻¹)	References
Rice straw	5 mg/50 mL	U	428.25	[131]
Rice straw	0.01g	U	242.65	[33]
Wheat straw	–	U	355.6	[82]
Rice husk	1	U	52.63	[125]
Rice husk	0.38	U	138.88	[81]
Rice husk	0.4	U	118	[132]
Corn cob	0.25	U	163.18	[34]
Pine needles	5	U	623.7	[37]
Pine needles	0.01 g/50 mL	U	62.7	[172]
Pine sawdust	0.2	U	514.72	[133]
Macaúba palm	10	U	488.7	[36]
Palm tree fibres	0.1 g	U	112	[121]
Bamboo sawdust	0.4	U	229.2	[111]
Bamboo biomass	–	U	274.15	[134]
Bamboo shoot shell	2	U	32.3	[105]
Cactus fibre	0.01	U	214	[118]
Camphor tree leaves	0.25	U	98.29	[173]
Miswak branches	1	U	85.71	[174]
Chinese banyan aerial root	1	U	27.29	[135]
Eucalyptus the Wood	5	U	27.2	[175]
Puncture vine	0.5g	U	17.24	[39]
Water hyacinth	0.2	U	138.57	[176]
Hydrophyte biomass	1	U	54.35	[136]
Hydrophyte	0.4	U	128.5	[137]
Switchgrass	0.1	U	4	[177]
Pig manure	0.3	U	979.3	[107]
Pig manure	0.3	U	661.7	[107]
Pig manure	0.1	U	952.5	[138]
Pig manure	–	U	221.4	[124]

Table 4. Cont.

Feedstock	Biochar Dose (g L ⁻¹)	Target Pollutant	Adsorption Capacity (mg g ⁻¹)	References
Horse manure	0.1	U	516.5	[108]
Horse manure	0.1	U	625.8	[139]
Cow manure	–	U	73.3	[82]
Carp fish scales	0.1	U	291.98	[122]
Sewage sludge	0.25	U	96.73	[34]
Sewage sludge	0.13	U	490.2	[140]
Winery waste (grape peels)	1	U	255	[141]
Winery waste (grape peels)	1	U	100	[141]
Malt spent rootlets	0.01	U	547	[120]
Coffee espresso residue	0.01	U	547	[120]
Olive kernels	0.01	U	357	[120]
Fungi	0.05	U	427.9	[142]
Green algae	0.5	U	100.2	[143]
Cyanobacteria	0.5	U	58.05	[144]
Sponge gourd	5 mg/50 mL	U	239.21	[83]
Sponge gourd fibres	–	U	904	[84]
Sponge gourd sponges	0.01 g	U	92	[119]
Sponge gourd sponge	–	U	833	[145]
Sponge gourd residue	0.4	U	382	[146]
Watermelon rind	1	U	323.56	[85]
Watermelon seeds	1	U	27.61	[38]
Longan shell (fruit)	0.1	U	331.13	[77]
Orange peel	10 mg/50 mL	U	246.3	[106]
Rice straw	1	F ⁻	111.11	[89]
Wheat straw	1	F ⁻	51.28	[90]
Rice husk	4	F ⁻	4.45	[178]
Rice husk	1	F ⁻	17.3	[24]
Rice husk	0.1	F ⁻	21.59	[150]
Rice husk	10	F ⁻	1.856	[149]
Black gram straw	2.5	F ⁻	16	[96]
Corn stover	5	F ⁻	4.11	[91]
Chir pine	2	F ⁻	16.72	[151]
Mongolian scotch pine tree sawdust	3.6 g/100 mL	F ⁻	0.885	[35]
Pine bark	10	F ⁻	9.77	[179]
Pine wood	10	F ⁻	7.66	[179]
Douglas fir (pine)	0.05 g/25 mL	F ⁻	9.04	[152]
Douglas fir (pine)	25 mg	F ⁻	36	[153]
Reed biomass	1	F ⁻	34.86	[128]
Kashgar tamarisk	5	F ⁻	164.23	[40]
Tea oil plant (seed shells)	1.6	F ⁻	11.04	[93]
Sawdust	5	F ⁻	4.413	[154]
Coconut	7	F ⁻	–	[92]
Cattail	–	F ⁻	1.28	[180]
Pongamia pinnata seed cake	10	F ⁻	1.11	[7]
Pomelo peel	2.5	F ⁻	18.52	[95]
Watermelon rind	0.2 g	F ⁻	9.5	[94]
Okra (lady finger) stem	2.5	F ⁻	20	[96]
Spent mushroom compost	2	F ⁻	4.7	[13]
Food waste	0.1 g/30 mL	F ⁻	123.4	[156]
Tea waste	10	F ⁻	52.5	[157]
Red algae seaweed	0.6 g/100 mL	F ⁻	2.1	[158]
Dairy manure	0.33	F ⁻	0.51	[109]
Sheep bone	1	F ⁻	2.33	[112]
Bone residues (chicken, cattle, and mixed bones)	1	F ⁻	4.29	[181]
Eggshell and platanus acerifoli leaves (5:1)	1.6	F ⁻	308	[97]

U: Uranium; F⁻: Fluoride; -: data not available.

De et al. [7] observed F⁻ concentrations of 5–20 mg L⁻¹ with a fixed biochar dose to examine the impact of initial concentration. The highest removal percentage of 98.5% was obtained at 10 mg L⁻¹ F⁻ concentration. However, with a further rise in the initial concentration, the adsorption decreased drastically because of the saturation of active surface sites. Mahmoud et al. [182] determined the influence of the initial concentration of uranyl ions in the range of 30–150 mg L⁻¹ at a constant pH, contact time, and dosage and found that the removal percentage increased from 81.3% to 89.5% for 30–80 mg L⁻¹ uranyl

ion concentration. However, increased uranyl ion concentration from 80 to 150 mg L⁻¹ decreased the removal efficiency due to more ions in the solution than the biochar surface active sites.

Table 5. Influence of initial concentration on adsorption of F⁻ and U.

Feedstock	Initial Conc. (mg L ⁻¹)	Target Pollutant	Adsorption Capacity (mg g ⁻¹)	References
Rice straw	6	F ⁻	111.11	[89]
Wheat straw	6	F ⁻	51.28	[90]
Rice husk	5	F ⁻	4.45	[178]
Rice husk	5	F ⁻	17.3	[24]
Rice husk	2	F ⁻	21.59	[150]
Rice husk	4	F ⁻	1.856	[149]
Black gram straw	10	F ⁻	16	[96]
Corn stover	100	F ⁻	4.11	[91]
Chir pine	50	F ⁻	16.72	[151]
Mongolian scotch pine tree sawdust	20	F ⁻	0.885	[35]
Pine bark	100	F ⁻	9.77	[179]
Pine wood	100	F ⁻	7.66	[179]
Douglas fir (pine)	10	F ⁻	9.04	[152]
Douglas fir (pine)	50	F ⁻	36	[153]
Reed biomass	10	F ⁻	34.86	[128]
Kashgar tamarisk	40	F ⁻	164.23	[40]
Tea oil plant (seed shells)	70	F ⁻	11.04	[93]
Sawdust	10	F ⁻	4.413	[154]
Coconut	10	F ⁻	–	[92]
Cattail	20	F ⁻	1.28	[180]
Pongamia pinnata seed cake	10	F ⁻	1.11	[7]
Pomelo peel	10	F ⁻	18.52	[132]
Watermelon rind	50	F ⁻	9.5	[94]
Okra (lady finger) stem	10	F ⁻	20	[96]
Spent mushroom compost	10	F ⁻	4.7	[13]
Food waste	300	F ⁻	123.4	[156]
Tea waste	50	F ⁻	52.5	[157]
Red algae seaweed	15	F ⁻	2.1	[158]
Dairy manure	5	F ⁻	0.42	[109]
Sheep bone	10	F ⁻	2.33	[112]
Bone residues (chicken, cattle and mixed bones)	10	F ⁻	4.29	[181]
Eggshell and platanus acerifoli leaves (5:1)	500	F ⁻	308	[97]
Rice straw	50	U	428.25	[131]
Rice straw	50	U	242.65	[33]
Wheat straw	10	U	355.6	[82]
Rice husk	10	U	52.63	[125]
Rice husk	3	U	138.88	[81]
Rice husk	80	U	118	[132]
Corn cob	25	U	163.18	[34]
Pine needles	11.9	U	623.7	[37]
Pine needles	50	U	62.7	[172]
Pine sawdust	10	U	514.72	[133]
Macaúba palm	5	U	488.7	[36]
Palm tree fibres	11.9	U	112	[121]
Bamboo sawdust	47.6	U	229.2	[111]
Bamboo biomass	–	U	274.15	[134]
Bamboo shoot shell	50	U	32.3	[105]
Cactus fibre	119	U	214	[118]
Camphor tree leaves	50	U	98.29	[173]
Miswak branches	60	U	85.71	[174]
Chinese banyan aerial root	30	U	27.29	[135]
Eucalyptus the Wood	300	U	27.2	[175]
Puncture vine	50	U	17.24	[39]
Water hyacinth	30	U	138.57	[176]
Hydrophyte biomass	–	U	54.35	[136]
Hydrophyte	47.6	U	128.5	[137]
Switchgrass	10	U	4	[177]
Pig manure	10	U	979.3	[107]
Pig manure	10	U	661.7	[107]
Pig manure	10	U	952.5	[138]

Table 5. Cont.

Feedstock	Initial Conc. (mg L ⁻¹)	Target Pollutant	Adsorption Capacity (mg g ⁻¹)	References
Pig manure	10	U	221.4	[124]
Horse manure	10	U	516.5	[108]
Horse manure	10	U	625.8	[139]
Cow manure	10	U	73.3	[82]
Carp fish scales	40	U	291.98	[122]
Sewage sludge	25	U	96.73	[34]
Sewage sludge	50	U	490.2	[140]
Winery waste (grape peels)	100	U	255	[141]
Winery waste (grape peels)	100	U	100	[141]
Malt spent rootlets	–	U	547	[120]
Coffee espresso residue	–	U	547	[120]
Olive kernels	–	U	357	[120]
Fungi	10	U	427.9	[142]
Green algae	50	U	100.2	[143]
Cyanobacteria	50	U	58.05	[144]
Sponge gourd	5	U	239.21	[83]
Sponge gourd fibres	–	U	904	[84]
Sponge gourd sponges	119	U	92	[119]
Sponge gourd sponge	–	U	833	[145]
Sponge gourd residue	225	U	382	[146]
Watermelon rind	20	U	323.56	[85]
Watermelon seeds	30	U	27.61	[38]
Longan shell (fruit)	23.6	U	331.13	[77]
Orange peel	50	U	246.3	[106]

U = Uranium, F⁻ = Fluoride, _ data not available.

3.7.4. Influence of Co-Existing Ions

Various ions from different sources, including sulphate, chloride, nitrate, carbonate, bicarbonate, phosphate, etc., are generally present in groundwater [13]. These ions were found to regulate the adsorption process by competing with U and F⁻ ions for interaction with the active surface sites of biochar. The presence of these anions decreased the adsorption efficiency. Liao et al. [107] reported a significant reduction in U adsorption due to the interference of Ca²⁺, Al³⁺, SO₄²⁻, CO₃²⁻, and PO₄³⁻ ions. Due to the large radius and high valency of Ca²⁺ and Al³⁺, U ions were easily captured by the biochar and occupied the active surface sites, leading to decreased U adsorption efficiency. SO₄²⁻, CO₃²⁻, and PO₄³⁻ formed stable complexes with U resulting in the reduction in adsorption efficiency of U. Mei et al. [93] observed the effect of SO₄²⁻, NO₃⁻, Cl⁻, and HCO₃⁻ on the F⁻ adsorption, where NO₃⁻, Cl⁻, and SO₄²⁻ had little impact on the F⁻ adsorption while HCO₃⁻ reduced the F⁻ adsorption due to the ion competition.

However, some studies have shown that the co-existing ions (Cl⁻, NO₃⁻, PO₄³⁻, and SO₄²⁻) had little or no significant impact on the adsorption efficiency of U and F⁻ due to their selectivity of biochar-based materials and their modification methods [13,85]. It was observed that the major co-existing ions interfering with the adsorption of U and F⁻ were phosphate, sulphate, carbonate, and bicarbonate. In addition, it depends on the properties of the feedstock chosen for the biochar and the materials and methods used for its modification which highly affect the adsorption efficiency of the biochar. Hence, it is crucial to know the co-existing ions in natural groundwater to improve the selectivity of adsorbent for the U and F⁻ removal experiments.

3.7.5. Influence of Pyrolysis Temperature on U and F⁻ Adsorption

Pyrolysis temperature is an essential factor influencing the quality and yield of biochar. The pyrolysis temperature mainly affects the structure and properties of the biochar. Table 6 shows the effect of pyrolysis temperature on U and F⁻ adsorption. Higher temperature increases the pH, surface area, and ash content of the biochar but reduces the yield of the biochar [69,70,74,100]. Furthermore, with the rise in temperature, the porosity of the biochar increases due to the removal of volatile matter, and porosity enhances the adsorptive capacity of biochar [69,74]. Biochar produced at higher temperatures possesses

a higher stable fraction than those prepared at lower temperatures [69]. Oxygen-containing functional groups, for example, carboxyl, hydroxyl, carbonyl, ether, and lactone, on the biochar decreases with an increase in temperature [69,183].

Table 6. Effect of carbonization temperature on U and F⁻ adsorption.

Feedstock	Carbonization Temp. (°C)	Surface Area (m ² g ⁻¹)	Target Pollutant	Adsorption Capacity (mg g ⁻¹)	References
Rice straw	500	157.96	U	428.25	[131]
Rice straw	500	–	U	242.65	[33]
Wheat straw	450	290.1	U	355.6	[82]
Rice husk	500	109.65	U	52.63	[125]
Rice husk	300	62.88	U	138.88	[81]
Rice husk	500	109	U	118	[132]
Corn cob	800	–	U	163.18	[34]
Pine needles	600	–	U	623.7	[37]
Pine needles	180	–	U	62.7	[172]
Pine sawdust	500	51.45	U	514.72	[133]
Macauá palm	350	643.12	U	488.7	[36]
palm tree fibres	650	–	U	112	[121]
Bamboo sawdust	450	1298	U	229.2	[111]
Bamboo biomass	700	445.17	U	274.15	[134]
Bamboo shoot shell	500	10.93	U	32.3	[105]
Cactus fibre	600	<5	U	214	[118]
Camphor tree leaves	350	65.91	U	98.29	[173]
Miswak branches	400	9.05	U	85.71	[174]
Chinese banyan aerial root	600	284	U	27.29	[135]
Eucalyptus wood	400	20	U	27.2	[175]
Puncture vine	500	–	U	17.24	[39]
Water hyacinth	400	50.545	U	138.57	[176]
Hydrophyte biomass	700	92.43	U	54.35	[136]
Hydrophyte	500	433	U	128.5	[137]
Switchgrass	300	2.9	U	4	[177]
Pig manure	500	–	U	979.3	[107]
Pig manure	500	–	U	661.7	[107]
Pig manure	500	227.9	U	952.5	[138]
Pig manure	250	–	U	221.4	[124]
Horse manure	500	–	U	516.5	[108]
Horse manure	500	–	U	625.8	[139]
Cow manure	450	101.5	U	73.3	[82]
Carp fish scales	330	1074.73	U	291.98	[122]
Sewage sludge	500	–	U	96.73	[34]
Sewage sludge	600	623.09	U	490.2	[140]
Winery waste (grape peels)	650	–	U	255	[141]
Winery waste (grape peels)	650	165	U	100	[141]
Malt spent rootlets (MSR)	850	540	U	547	[120]
Coffee espresso residue	850	700	U	547	[120]
Olive kernels	850	510	U	357	[120]
Fungi	160	102.7	U	427.9	[142]
Green algae	180	63.7	U	100.2	[143]
Cyanobacteria	200	–	U	58.05	[144]
Sponge gourd	400	–	U	239.21	[83]
Sponge gourd fibres	650	<5	U	904	[84]
Sponge gourd sponges	650	–	U	92	[119]
Sponge gourd sponge	650	–	U	833	[145]
Sponge gourd residue	200	–	U	382	[146]
Watermelon rind	500	86.35	U	323.56	[85]
Watermelon seeds	350	–	U	27.61	[38]
Longan shell (fruit)	800	1168.88	U	331.13	[77]
Orange peel	650	273.25	U	246.3	[106]
rice straw	500	95.36	F ⁻	111.11	[89]
Wheat straw	–	–	F ⁻	51.28	[90]
Rice husk	700	58.98	F ⁻	4.45	[178]
Rice husk	600	–	F ⁻	17.3	[24]
Rice husk	600	114	F ⁻	21.59	[150]
Rice husk	500	2.45	F ⁻	1.856	[149]
Black gram straw	500	9.27	F ⁻	16	[96]
Corn stover	500	3.61	F ⁻	4.11	[91]
Chir pine	400	–	F ⁻	16.72	[151]
Mongolian scotch pine tree sawdust	550	339	F ⁻	0.885	[35]
Pine bark	450	1.88	F ⁻	9.77	[179]
Pine wood	450	2.73	F ⁻	7.66	[179]
Douglas fir (pine)	1000	494	F ⁻	9.04	[152]
Douglas fir (pine)	1000	576	F ⁻	36	[153]
Reed biomass	600	236.84	F ⁻	34.86	[128]
Kashgar tamarisk	350	164.52	F ⁻	164.23	[40]
Tea oil plant (seed shells)	400	–	F ⁻	11.04	[93]
Sawdust	660	57.97	F ⁻	4.413	[154]
Pongamia pinnata seed cake	550	10.1	F ⁻	1.11	[7]
Coconut	700	1054	F ⁻	–	[92]

Table 6. Cont.

Feedstock	Carbonization Temp. (°C)	Surface Area (m ² g ⁻¹)	Target Pollutant	Adsorption Capacity (mg g ⁻¹)	References
Cattail	800	733.62	F ⁻	1.28	[180]
Pomelo peel	600	–	F ⁻	18.52	[132]
Watermelon rind	400	0.5365	F ⁻	9.5	[94]
Okra (lady finger) stem	600	23.52	F ⁻	20	[96]
Spent mushroom compost	500	28.5	F ⁻	4.7	[13]
Food waste	600	20.95	F ⁻	123.4	[156]
Tea waste	400	11.833	F ⁻	52.5	[157]
Red algae seaweed	450	319.47	F ⁻	2.1	[158]
Dairy manure	500	2.6	F ⁻	0.42	[109]
Sheep bone	650	113.874	F ⁻	2.33	[112]
Bone residues (chicken, cattle, and mixed bones)	350	–	F ⁻	4.29	[181]
Bone residues (chicken, cattle, and mixed bones)	700	–	F ⁻	2.91	[181]
Eggshell and platanus acerifoli leaves (5:1)	800	44.7	F ⁻	308	[97]

U = Uranium, F⁻ = Fluoride, – not available.

3.7.6. Influence of Different Feedstocks on U and F⁻ Adsorption

Several feedstocks have been utilized to prepare biochar to remove U and F⁻ from aqueous solution. For example, magnetically modified rice husk biochar was prepared by Wang et al. [132] to remove U. Magnetization enhanced the biochar surface area from 52.1 m² g⁻¹ to 109 m² g⁻¹ and pore volume from 0.02 cm³ g⁻¹ to 0.05 cm³ g⁻¹, thereby increasing U adsorption capacity from 64 mg g⁻¹ (raw biochar) to 118 mg g⁻¹ (modified biochar) (Table 1) at pH 7 and temperature of 55 °C. Similar findings were reported by [37,39,85,125,136]. Similarly, phosphate-impregnated biochar from bamboo biomass was examined for U removal. Biochar fabrication increased the surface area from 10.31 m² g⁻¹ to 445.17 m² g⁻¹ and pore volume from 0.031 m³ g⁻¹ to 0.236 m³ g⁻¹, which resulted in enhanced U adsorption potential from 15.869 mg g⁻¹ to 274.15 mg g⁻¹ at pH 4 and a temperature of 25 °C [134]. Ying et al. [106] applied orange-peel-derived biochar modified with MnO₂ for U extraction. MnO₂ modification increased the surface area of the biochar from 165.01 m² g⁻¹ to 273.25 m² g⁻¹ and improved the U sorption ability of biochar from 165.4 mg g⁻¹ to 246.3 mg g⁻¹. Similar results were observed by [84]. Dairy-manure-based biochar was used for the defluoridation of water. The prepared biochar was modified with calcium, and modified biochar showed 75% removal efficiency with a F⁻ uptake of 0.11 mg g⁻¹ for pristine biochar and 0.42 mg g⁻¹ for modified biochar at pH 8 and a temperature of 25 °C [109].

3.8. Adsorption Mechanism of U and F⁻

The physical and chemical reactions between adsorbate (U, F⁻) and adsorbent (biochar) regulate U and F⁻ removal from an aqueous solution. Adsorption mechanisms differ according to the type of biomass or feedstock, the presence of functional groups on biochar surface, the physicochemical properties of biochar such as the pH of the medium, and the type of target contaminants [47,57]. Figure 5 summarizes the major adsorption mechanisms of U and F⁻ on biochar. The possible adsorption mechanisms for U and F⁻ are ion exchange, surface complexation, electrostatic attraction, and precipitation.

The most probable adsorption mechanisms of F⁻ and U are ion exchange, electrostatic interactions, and surface complexation. Ion exchange is the interaction between the oxygen-based functional groups on the biochar surface and the target contaminant, which involves exchanging the same type of ions (cation–cation or anion–anion). In the case of F⁻ adsorption, ion exchange is associated with ion replacement in which F⁻ ions replace an ion (hydroxyl, carboxylic, and sulphate) from biochar surface [35,82,83,90,127,128,131,132]. For instance, Mei et al. [93] removed the F⁻ from water using zirconium dioxide biochar through ion exchange between OH⁻ and F⁻ on the zirconia particles. Wang et al. [95] used polypyrrole-modified biochar synthesized from pomelo peel to remove F⁻ and concluded that ion exchange (anion exchange between F⁻ and Cl⁻) was the main adsorption mechanism.

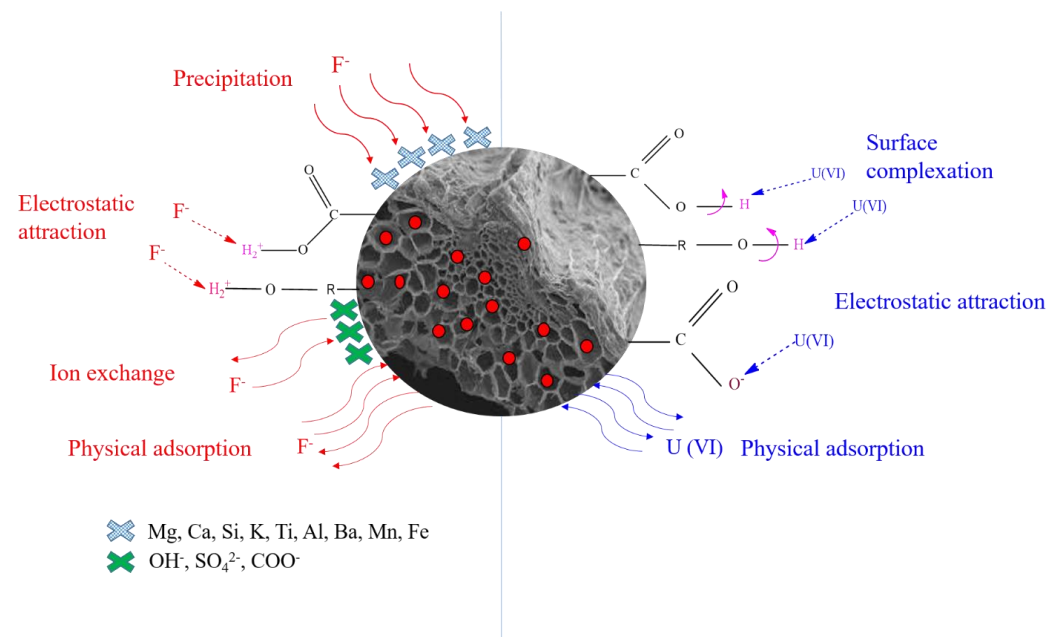


Figure 5. Schematic representation of major mechanisms of U and F^- adsorption on biochar surface.

Electrostatic interaction occurs between the oppositely charged surface of biochar and contaminants. Electrostatic interaction is related to the solution pH and the pH_{PZC} of the biochar. When the solution $pH < pH_{PZC}$, the surface charge of the biochar becomes positive and binds the anionic contaminants. When the $pH > pH_{PZC}$, the biochar surface is negatively charged and binds the cationic contaminants [51,56]. For instance, Sadhu et al. [94] found that maximum adsorption of F^- was at pH 1 because the pH_{PZC} of biochar was at pH 2.1. Electrostatic interactions also occurred between the negative- and positive-charged biochar and U, F^- as a result of ionization of the functional groups, such as $-COOH_2^+$, $-ROH_2^+$, or $-COO^-$ [56,94,107]. Surface complexation (inner sphere and outer sphere) involves the adsorption of U and F^- through the formation of complexes with oxygen functional groups, such as carboxyl, hydroxyl, and carbonyl [31]. Many studies revealed that the dominant mechanism for U adsorption was surface complexation between U(VI) ions and the surface functional groups $-COOH$, $-OH$, $-CO$ [33,34,37–39,85,119,132]. Metal F^- precipitation is another mechanism suggested for F^- adsorption, which involves the presence of metals, such as Ca, Mg, Si, K, Al, Mn, Ba, Fe, and Ti in biochar, and F^- ions react with these metals to form insoluble fluorides on biochar [94,97,179].

4. Adsorption Isotherms, Kinetics, and Thermodynamics

4.1. Adsorption Isotherms

The Langmuir and Freundlich isotherm models are generally used to evaluate the equilibrium adsorption capacity of U and F^- . The Langmuir isotherm shows the homogeneous adsorption process and monolayer adsorption, while the Freundlich model shows heterogeneity and multilayer adsorption. For example, Chen et al. [133] assessed the interaction between initial U concentration and equilibrium adsorption capacity. They reported that the Langmuir adsorption isotherm was more favourable for describing the U adsorption than other models and confirmed that the adsorption process is single-layer adsorption. Similarly, Meilani et al. [156] performed an isotherm study to detect the F^- adsorption and adsorption capacity of aluminium-modified food waste biochar. It was found that sorption occurred by the Langmuir adsorption isotherm, which suggested that adsorption was monolayer, homogeneous, occurred only on localized sites, and there were no interactions between the adsorbed ions. In another study, Dai et al. [34] applied the Langmuir and Freundlich isotherm models to assess the U adsorption capacity of corn cob biochar (CCB) and sewage sludge biochar (SSB). They found that the Langmuir isotherm model better

fitted U adsorption by CCB while the Freundlich isotherm model better fitted U adsorption by SSB. Since the CCB was ash-poor biochar, the surface structure was homogeneous, while SSB was ash-rich biochar; thus, the surface structure was heterogeneous.

However, in some cases, the Tempkin and Halsey adsorption isotherm model is also used. For instance, Sadhu et al. [94] applied four adsorption isotherm models (including Langmuir, Freundlich, Tempkin, and Halsey) to depict the F^- adsorption and found that experimental data were better fitted by the Freundlich model than the other three models. Halsey isotherm is appropriate for multilayer adsorption, and Tempkin isotherm is suitable for the uniform distribution of binding energies.

4.2. Adsorption Kinetics

Adsorption kinetics is used to analyse the adsorption behaviour between biochar and contaminants (U and F^-) with reference to contact time. Pseudo-first-order and pseudo-second-order kinetic models were used to investigate U and F^- adsorption on the biochar. For instance, Chen et al. [133] reported that the adsorption behaviour between U and MgO/biochar was chemisorption because the correlation coefficient (R^2) of pseudo-second-order kinetics was greater than the first-order kinetics. Similarly, Meilani et al. [156] employed pseudo-first-order and pseudo-second-order models to examine the adsorption mechanism of F^- on the surface of aluminium-modified food waste biochar. They found that the adsorption process was chemical adsorption, as pseudo-second-order kinetics fitted better with the experimental data due to the higher regression coefficient (R^2) than the pseudo-first-order model. In another study, Dai et al. [34] performed adsorption kinetics and concluded that the U adsorption process was both physical and chemical adsorption. It was found that the U adsorption process involved two steps: first, the initial phase, which contained rapid adsorption, and second, it involved a slower adsorption process. In the initial rapid phase, a higher amount of U adsorbed onto the CCB (ash-poor), and a lower amount of U adsorbed on the SSB (ash-rich) in the later slower phase. It was found that pseudo-first-order and pseudo-second-order models both fitted well for U adsorption process.

4.3. Adsorption Thermodynamics

Adsorption thermodynamics is used to analyse the adsorption process with respect to temperature. The thermodynamic factors, including enthalpy, Gibbs free energy, and entropy, provide information about the adsorption process. Negative Gibbs free energy represents that the adsorption process increases with respect to temperature and is spontaneous. Negative enthalpy indicates that adsorption capacity decreases with an increase in temperature, and the process of adsorption is heat-releasing. The positive enthalpy value shows that the adsorption potential increases with the rise in temperature, and the process is heat-absorbing. The positive entropy value represents the rise in randomness at the liquid–solid mass transfer interface. For example, Chen et al. [133] reported that the U adsorption process by MgO/biochar was spontaneous and exothermic because the adsorption capability declined with the rising temperature, which confirmed that the sorption process was exothermic and negative Gibbs free energy described the spontaneity of the process. In another study, Guan et al. [35] reported that F^- adsorption on modified Mongolian scotch pine tree sawdust biochar increased with respect to temperature ($T = 308, 318, \text{ and } 328 \text{ K}$), which indicated that the adsorption process was endothermic. Similarly, Ahmed et al. [39] examined the influence of temperature on the sorption process of U on the magnetized biochar derived from *Tribulus terrestris* plant. They found that the sorption process was spontaneous and heat-absorbing because U adsorption increased with rising temperature from 298 to 318 K with negative Gibbs free energy and positive enthalpy and entropy.

5. Regeneration of Biochar

Regeneration of biochar is the reverse of the adsorption process achieved by desorbing the contaminant from the biochar. It improves the reusability and stability of the biochar by performing sorption/desorption cycles. Desorption experiments were performed using desorbing agents, mainly acids and alkaline solutions. For instance, Mishra et al. [175] studied the desorption of the U from loaded biochar using nitric acid. They reported that acids are better eluting agents because they provide H^+ ions which tend to protonate the surface of biochar, resulting in the elution of positively charged U ions. In another investigation, Liao et al. [138] examined the reusability of pig-manure-derived biochar using ethanol, HCl, KOH, and deionized water as desorbing agents. Among them, HCl showed the effective desorption of U because, at low pH, hydronium ions have more affinity for active sites than the U(VI) species. The removal efficiency was found to be 85% after five cycles. Pang et al. [142] tested the stability and reusability of nano-zerovalent iron-based biochar. They performed five regeneration cycles using sodium bicarbonate as a desorbing agent to desorb U. They reported that the removal efficiency of biochar was 80.6% in the first cycle, which declined to 52% after five cycles.

Various U(VI) sorption–desorption cycles were performed by Philippou et al. [37], who found that the adsorption capability of the biochar for U decreased after each cycle due to the loss of biochar material. Adsorption % declined from 99.5 to 87.2%, and desorption% reduced from 99.6 to 62.6% after four cycles. Sadhu et al. [94] performed three cycles of sorption–desorption to analyse the desorption of F^- from watermelon rind biochar and concluded that the adsorption capacity of biochar was 79.54% after the first cycle, 71.99% after the second cycle, and 60.17% after the third cycle. Hence, the prepared biochar was stable and could be reused. Similarly, De et al. [7] examined the reusability of biochar using H_2SO_4 desorbing agent to desorb F^- . They performed five cycles of sorption–desorption and reported an adsorption percentage of 98.5% after the first cycle and 68% after five cycles. Ahmed et al. [39] assessed the reusability of biochar by performing five cycles of repeated adsorption of U on magnetic biochar obtained from a *Tribulus terrestris* plant. It was found that the adsorption potential of biochar slightly declined after five cycles suggesting that the biochar has the potential to extract U from water and can be reused.

6. Challenges and Limitations for Real U and F^- Groundwater Treatment

The application of biochar for treating real U and F^- -contaminated groundwater is crucial for understanding the practical applicability and limitations of low-cost novel adsorbents. Lingamdinne et al. [85] have tested real groundwater spiked with 10 mg L^{-1} of U from Republic of Korea for U treatment using magnetic watermelon rind biochar. In semi-column experiments, more than 90% of U was removed with magnetic biochar in up to three cycles at pH 4. In addition, Sen et al. [81] collected groundwater from West Bengal and Jharkhand, with U concentrations in the range of $38\text{--}85\ \mu\text{g L}^{-1}$. Therefore, iron-modified biochar showed a maximum removal efficiency of 97–99.77% for U at pH 5.5–8.0 at $< 1\text{ g}$ of biochar dose. Interestingly, in the USA, Kumar et al. [177] collected groundwater with pH 3.9 and U concentrations of 3.0 mg L^{-1} , which reported an adsorption capacity of 0.52 mg g^{-1} using switchgrass biochar in column experiments. Through batch sorption experiments, the adsorption capacity for U was observed at 2.12 mg g^{-1} at pH 3.9, whereas it increased to about 4 mg g^{-1} with increasing pH up to 5.9 [177]. From the above analysis, it has been clear that U removal from real groundwater is pH-dependent, and the effect of biochar dose, initial U concentration, and other dependent parameters is yet to be investigated.

Recently, Kumar et al. [184] have summarized practical applications and limitations in treating F^- -contaminated water through raw/modified biochar. It has been investigated that most of the research has been performed at low pH to treat real or spiked groundwater using biochars. For example, Mohan et al. [91] have reported that low adsorption capacity, 4.38 and 5.37 mg L^{-1} , was observed at pH 2 using corn stover pristine biochar and magnetic biochar, respectively, for 10 mg L^{-1} fluorides-spiked groundwater collected

from Ghaziabad, India. In the context of industrial effluents, Sadhu et al. [94] have treated industrial wastewater with F^- concentrations of 5570 mg L^{-1} in multiple batch runs with increasing biochar dosage at pH 1 using watermelon rind biochar. In contrast, few studies have also treated F^- -contaminated groundwater close to neutral pH (5–8) with a removal efficiency of 81–100% [92,185,186]. For example, Zhou et al. [186] observed that 100% F^- removal efficiency was removed from groundwater having 5 mg L^{-1} F^- concentrations using magnetic biochar at pH 8. Similarly, a removal efficiency of 81% was observed for F^- -contaminated groundwater with 7 mg L^{-1} using shell-derived activated biochar at pH 6.5 [92]. In addition, in China, 97% of F^- -contaminated groundwater (9.8 mg L^{-1}) was treated with lanthanum-modified biochar at pH 5.2 [185]. Besides adsorption, the gravity filtration method showed a removal efficiency of 92.5–94.7% for F^- ions from drinking water using iron-modified biochar [187]. Apart from this, groundwater contains various cations/anions that can significantly influence F^- removal during the treatment of real groundwater using biochar, which is yet to be investigated. Batch sorption experiments were extensively performed using raw/modified biochar at the laboratory scale; however, very few studies have reported the implication of biochars in column experiments to treat F^- -contaminated water. The transport and deposition of F^- were analysed with respect to adsorbent dosage, F^- concentrations, and flow velocity, as these parameters can impact F^- adsorption. For example, the retention and transport mechanism for F^- in column experiments, using various biochars derived, such as pulse straw biochar [96], modified biochar (MgO-biochar) [155], and dairy manure-derived biochar [109].

Till now, biochar research has mostly been carried out at a small scale/laboratory scale. So, to upscale biochar for the treatment of natural groundwater/wastewater/surface water, the major limitations include controlled experimental designs in the laboratory, which is the main limiting factor while implementing biochar at a large scale. Most of the experiments are batch experiments, with limited column studies. The cost of production is one of the major factors limiting biochar application on a large scale. There are limited studies on removing U and F^- from real aquifers/surface water. There are operational challenges while designing a water treatment plant to remove U and F^- using biochar. Natural groundwater/surface waters contain co-existing ions with respect to U and F^- , which interferes with the adsorption. A risk assessment of biochar application needs to be investigated to remove U and F^- from drinking water. The toxicological impacts of biochar need to be investigated. Biochar recycling and management of the waste biochar need to be taken into consideration. There are studies related to the regeneration and reusability of biochar, but the efficiency of the biochar decreases after a few cycles. Hence, the safe disposal and alternate use of waste biochar are the concern.

7. Conclusions, Research Gaps, and Future Perspectives

The present review has summarized the recent studies for removing U and F^- from aqueous solution using raw and modified biochar prepared from different feedstocks. Different feedstocks, production techniques, modification methods, adsorption mechanisms, factors influencing the U and F^- adsorption, and experimental conditions for the optimum removal of U and F^- were reviewed in this paper. It was found that pyrolysis was the dominant biochar production technique. Low-to-medium pyrolysis temperature, cellulose, and hemicellulose-rich feedstocks such as crop residues, grasses, softwood, and manure-based biochars were effective for U and F^- removal. Acidic and magnetic modification favoured U adsorption, while metal oxides, hydroxides, and alkali modification aided F^- adsorption. The dominated adsorption mechanisms for U adsorption were surface complexation (inner-sphere complexation) and electrostatic attraction, whereas ion exchange, electrostatic attraction, and precipitation were adsorptive mechanisms for F^- ions. Different parameters affected the adsorption process, including pH, biochar dosage, initial concentration, co-existing ions, and pyrolysis temperature. It was found that alkaline pH facilitated F^- adsorption while slightly acidic and near-neutral pH favoured U adsorption. High pyrolysis temperature raised the pH of biochar and reduced the biochar yield.

Consequently, adsorption capacity decreased due to pore shrinking or pore breakage and loss of acidic functional groups. It is crucial to have knowledge about the co-existing ions in natural groundwater to improve the selectivity of adsorbent for the U and F^- removal experiments. Although several investigations have been carried out to remove U and F^- with biochar, some research gaps in the literature need to be addressed.

1. Most of the investigations have been carried out at lab scale through batch studies using synthetic water or simulated water, and limited studies have been performed using natural water. In order to scale up, column studies should be conducted for field applications, and future research should be focused on the treatment of natural water.
2. Most studies have focused on the selective removal/extraction of either U or F^- using biochar. However, actual waters contain multiple contaminants, so future research should focus on using biochar to remove multiple contaminants from water.
3. There is a lack of studies for the treatment of drinking-water sources such as natural waters and groundwater using biochar. Most of the studies have focused on the remediation of wastewater.
4. Most of the modifications are chemical modifications, and there is a need for environmentally friendly green methods/materials for modification.
5. The effect of co-existing ions has not been studied in detail. There is no detailed study on the impact of multiple components in the solution that interferes with the U and F^- adsorption.
6. Most studies have considered U as a cation (UO_2^{2+}), but in alkaline solutions, U exists as $(UO_2)_2CO_3(OH)^{3-}$ (anion). So, there is no study for treating anionic U using biochar from aqueous solution.

Author Contributions: Conceptualization, A.T. and P.K.S.; methodology, A.T.; formal analysis, A.T.; investigation, data curation, A.T.; writing—original draft preparation, A.T.; writing—review and editing, P.K.S. and R.K.; supervision, P.K.S. All authors have read and agreed to the published version of the manuscript.

Funding: This research was financially supported by the University Grants Commission (UGC) in the form of Ph.D. fellowship.

Data Availability Statement: Not applicable.

Acknowledgments: The first author would like to acknowledge the University Grants Commission (UGC), India for providing financial support in the form of Ph.D. fellowship. We acknowledge the DST-FIST (Fund for Improvement of S & T Infrastructure of the Department of Science and Technology) support at the Department of Environmental Science and Technology of the Central University of Punjab for providing support to this work. PKS would also like to acknowledge the SERB Core Research Grant (CRG/2021/002567) from the Department of Science and Technology (DST), India, and the Research Seed Money Grant (GP-25) from the Central University of Punjab for technical support.

Conflicts of Interest: The authors declare no conflict of interest.

References

1. Salehi, M. Global Water Shortage and Potable Water Safety; Today's Concern and Tomorrow's Crisis. *Environ. Int.* **2022**, *158*, 106936. [[CrossRef](#)] [[PubMed](#)]
2. Hering, J.G.; Maag, S.; Schnoor, J.L. A Call for Synthesis of Water Research to Achieve the Sustainable Development Goals by 2030. *Environ. Sci. Technol.* **2016**, *50*, 6122–6123. [[CrossRef](#)] [[PubMed](#)]
3. Aravinthasamy, P.; Karunanidhi, D.; Subramani, T.; Anand, B.; Roy, P.D.; Srinivasamoorthy, K. Fluoride Contamination in Groundwater of the Shanmuganadhi River Basin (South India) and Its Association with Other Chemical Constituents Using Geographical Information System and Multivariate Statistics. *Chem. Erde* **2020**, *80*, 125555. [[CrossRef](#)]
4. Kaur, G.; Kumar, R.; Mittal, S.; Sahoo, P.K.; Vaid, U. Ground/Drinking Water Contaminants and Cancer Incidence: A Case Study of Rural Areas of South West Punjab, India. *Hum. Ecol. Risk Assess.* **2021**, *27*, 205–226. [[CrossRef](#)]
5. Coyte, R.M.; Singh, A.; Furst, K.E.; Mitch, W.A.; Vengosh, A. Co-Occurrence of Geogenic and Anthropogenic Contaminants in Groundwater from Rajasthan, India. *Sci. Total Environ.* **2019**, *688*, 1216–1227. [[CrossRef](#)]

6. Ma, M.; Wang, R.; Xu, L.; Xu, M.; Liu, S. Emerging Health Risks and Underlying Toxicological Mechanisms of Uranium Contamination: Lessons from the Past Two Decades. *Environ. Int.* **2020**, *145*, 106107. [[CrossRef](#)]
7. De, D.; Santosha, S.; Aniya, V.; Sreeramoju, A.; Satyavathi, B. Assessing the Applicability of an Agro-Industrial Waste to Engineered Bio-Char as a Dynamic Adsorbent for Fluoride Sorption. *J. Environ. Chem. Eng.* **2018**, *6*, 2998–3009. [[CrossRef](#)]
8. Balaram, V.; Rani, A.; Rathore, D.P.S. Uranium in Groundwater in Parts of India and World: A Comprehensive Review of Sources, Impact to the Environment and Human Health, Analytical Techniques, and Mitigation Technologies. *Geosystems Geoenvironment* **2022**, *1*, 100043. [[CrossRef](#)]
9. Coyte, R.M.; Jain, R.C.; Srivastava, S.K.; Sharma, K.C.; Khalil, A.; Ma, L.; Vengosh, A. Large-Scale Uranium Contamination of Groundwater Resources in India. *Environ. Sci. Technol. Lett.* **2018**, *5*, 341–347. [[CrossRef](#)]
10. Brugge, D.; Buchner, V. Health Effects of Uranium: New Research Findings. *Rev. Environ. Health* **2011**, *26*, 231–249. [[CrossRef](#)]
11. Ali, S.; Thakur, S.K.; Sarkar, A.; Shekhar, S. Worldwide Contamination of Water by Fluoride. *Environ. Chem. Lett.* **2016**, *14*, 291–315. [[CrossRef](#)]
12. Kumar, M.; Goswami, R.; Patel, A.K.; Srivastava, M.; Das, N. Scenario, Perspectives and Mechanism of Arsenic and Fluoride Co-Occurrence in the Groundwater: A Review. *Chemosphere* **2020**, *249*, 126126. [[CrossRef](#)] [[PubMed](#)]
13. Chen, G.J.; Peng, C.Y.; Fang, J.Y.; Dong, Y.Y.; Zhu, X.H.; Cai, H.M. Biosorption of Fluoride from Drinking Water Using Spent Mushroom Compost Biochar Coated with Aluminum Hydroxide. *Desalin. Water Treat.* **2016**, *57*, 12385–12395. [[CrossRef](#)]
14. Shen, J.; Schäfer, A. Removal of Fluoride and Uranium by Nanofiltration and Reverse Osmosis: A Review. *Chemosphere* **2014**, *117*, 679–691. [[CrossRef](#)] [[PubMed](#)]
15. Katsoyiannis, I.A.; Zouboulis, A.I. Removal of Uranium from Contaminated Drinking Water: A Mini Review of Available Treatment Methods. *Desalin. Water Treat.* **2013**, *51*, 2915–2925. [[CrossRef](#)]
16. Bhatnagar, A.; Kumar, E.; Sillanpää, M. Fluoride Removal from Water by Adsorption—A Review. *Chem. Eng. J.* **2011**, *171*, 811–840. [[CrossRef](#)]
17. Ghosh, D.; Sinha, M.K.; Purkait, M.K. A Comparative Analysis of Low-Cost Ceramic Membrane Preparation for Effective Fluoride Removal Using Hybrid Technique. *Desalination* **2013**, *327*, 2–13. [[CrossRef](#)]
18. Ndiaye, P.I.; Moulin, P.; Dominguez, L.; Millet, J.C.; Charbit, F. Removal of Fluoride from Electronic Industrial Effluent by RO Membrane Separation. *Desalination* **2005**, *173*, 25–32. [[CrossRef](#)]
19. Azbar, N.; Türkman, A. Defluoridation in Drinking Waters. *Water Sci. Technol.* **2000**, *42*, 403–407. [[CrossRef](#)]
20. Chaturvedi, A.K.; Yadava, K.P.; Pathak, K.C.; Singh, V.N. Defluoridation of Water by Adsorption on Fly Ash. *Water. Air. Soil Pollut.* **1990**, *49*, 51–61. [[CrossRef](#)]
21. Habuda-Stanić, M.; Ravančić, M.; Flanagan, A. A Review on Adsorption of Fluoride from Aqueous Solution. *Materials* **2014**, *7*, 6317–6366. [[CrossRef](#)] [[PubMed](#)]
22. Samarghandi, M.R.; Khiadani, M.; Foroughi, M.; Zolghadr Nasab, H. Defluoridation of Water Using Activated Alumina in Presence of Natural Organic Matter via Response Surface Methodology. *Environ. Sci. Pollut. Res.* **2016**, *23*, 887–897. [[CrossRef](#)] [[PubMed](#)]
23. Vithanage, M.; Bhattacharya, P. Fluoride in the Environment: Sources, Distribution and Defluoridation. *Environ. Chem. Lett.* **2015**, *13*, 131–147. [[CrossRef](#)]
24. Goswami, R.; Kumar, M. Removal of Fluoride from Aqueous Solution Using Nanoscale Rice Husk Biochar. *Groundw. Sustain. Dev.* **2018**, *7*, 446–451. [[CrossRef](#)]
25. Arfin, T.; Waghmare, S. Fluoride Removal from Water by Mixed Metal Oxide Adsorbent Materials: A State-of-the-Art Review. *Int. J. Eng. Sci. Res. Technol.* **2015**, *4*, 519–536.
26. Velazquez-Jimenez, L.H.; Vences-Alvarez, E.; Flores-Arciniega, J.L.; Flores-Zuñiga, H.; Rangel-Mendez, J.R. Water Defluoridation with Special Emphasis on Adsorbents-Containing Metal Oxides and/or Hydroxides: A Review. *Sep. Purif. Technol.* **2015**, *150*, 292–307. [[CrossRef](#)]
27. Shuib, X.; Chun, Z.; Xinghuo, Z.; Jing, Y.; Xiaojian, Z.; Jingsong, W. Removal of Uranium (VI) from Aqueous Solution by Adsorption of Hematite. *J. Environ. Radioact.* **2009**, *100*, 162–166. [[CrossRef](#)]
28. Camacho, L.M.; Deng, S.; Parra, R.R. Uranium Removal from Groundwater by Natural Clinoptilolite Zeolite: Effects of PH and Initial Feed Concentration. *J. Hazard. Mater.* **2010**, *175*, 393–398. [[CrossRef](#)]
29. Alahabadi, A.; Singh, P.; Raizada, P.; Anastopoulos, I.; Sivamani, S.; Dotto, G.L.; Landarani, M.; Ivanets, A.; Kyzas, G.Z.; Hosseini-Bandegharai, A. Activated Carbon from Wood Wastes for the Removal of Uranium and Thorium Ions through Modification with Mineral Acid. *Colloids Surf. A Physicochem. Eng. Asp.* **2020**, *607*, 125516. [[CrossRef](#)]
30. (Ölmez) Aytaş, Ş.; Akyil, S.; Aslani, M.A.A.; Aytakin, U. Removal of Uranium from Aqueous Solutions by Diatomite (Kieselguhr). *J. Radioanal. Nucl. Chem.* **1999**, *240*, 973–976. [[CrossRef](#)]
31. Inyang, M.I.; Gao, B.; Yao, Y.; Xue, Y.; Zimmerman, A.; Mosa, A.; Pullammanappallil, P.; Ok, Y.S.; Cao, X. A Review of Biochar as a Low-Cost Adsorbent for Aqueous Heavy Metal Removal. *Crit. Rev. Environ. Sci. Technol.* **2016**, *46*, 406–433. [[CrossRef](#)]
32. Ahmad, M.; Rajapaksha, A.U.; Lim, J.E.; Zhang, M.; Bolan, N.; Mohan, D.; Vithanage, M.; Lee, S.S.; Ok, Y.S. Biochar as a Sorbent for Contaminant Management in Soil and Water: A Review. *Chemosphere* **2014**, *99*, 19–33. [[CrossRef](#)] [[PubMed](#)]
33. Ahmed, W.; Mehmood, S.; Qaswar, M.; Ali, S.; Khan, Z.H.; Ying, H.; Chen, D.Y.; Núñez-Delgado, A. Oxidized Biochar Obtained from Rice Straw as Adsorbent to Remove Uranium (VI) from Aqueous Solutions. *J. Environ. Chem. Eng.* **2021**, *9*, 105104. [[CrossRef](#)]

34. Dai, L.; Li, L.; Zhu, W.; Ma, H.; Huang, H.; Lu, Q.; Yang, M.; Ran, Y. Post-Engineering of Biochar via Thermal Air Treatment for Highly Efficient Promotion of Uranium(VI) Adsorption. *Bioresour. Technol.* **2020**, *298*, 122576. [[CrossRef](#)] [[PubMed](#)]
35. Guan, X.; Zhou, J.; Ma, N.; Chen, X.; Gao, J.; Zhang, R. Studies on Modified Conditions of Biochar and the Mechanism for Fluoride Removal. *Desalin. Water Treat.* **2015**, *55*, 440–447. [[CrossRef](#)]
36. Guilhen, S.N.; Rovani, S.; de Araujo, L.G.; Tenório, J.A.S.S.; Mašek, O. Uranium Removal from Aqueous Solution Using Macauba Endocarp-Derived Biochar: Effect of Physical Activation. *Environ. Pollut.* **2021**, *272*, 116022. [[CrossRef](#)] [[PubMed](#)]
37. Philippou, K.; Anastopoulos, I.; Dosche, C.; Pashalidis, I. Synthesis and Characterization of a Novel Fe₃O₄-Loaded Oxidized Biochar from Pine Needles and Its Application for Uranium Removal. Kinetic, Thermodynamic, and Mechanistic Analysis. *J. Environ. Manage.* **2019**, *252*, 109677. [[CrossRef](#)] [[PubMed](#)]
38. Ahmed, W.; Mehmood, S.; Núñez-Delgado, A.; Ali, S.; Qaswar, M.; Khan, Z.H.; Ying, H.; Chen, D.Y. Utilization of Citrullus Lanatus L. Seeds to Synthesize a Novel MnFe₂O₄-Biochar Adsorbent for the Removal of U(VI) from Wastewater: Insights and Comparison between Modified and Raw Biochar. *Sci. Total Environ.* **2021**, *771*, 144955. [[CrossRef](#)]
39. Ahmed, W.; Mehmood, S.; Núñez-delgado, A.; Qaswar, M.; Ali, S.; Ying, H.; Liu, Z.; Mahmood, M.; Chen, D. Fabrication, Characterization and U (VI) Sorption Properties of a Novel Biochar Derived from Tribulus Terrestris via Two Different Approaches. *Sci. Total Environ.* **2021**, *780*, 146617. [[CrossRef](#)]
40. Habibi, N.; Rouhi, P.; Ramavandi, B. Modification of Tamarix Hispida Biochar by Lanthanum Chloride for Enhanced Fluoride Adsorption from Synthetic and Real Wastewater. *Environ. Prog. Sustain. Energy* **2019**, *38*, S298–S305. [[CrossRef](#)]
41. Liang, L.; Xi, F.; Tan, W.; Meng, X.; Hu, B.; Wang, X. Review of Organic and Inorganic Pollutants Removal by Biochar and Biochar-Based Composites. *Biochar* **2021**, *3*, 255–281. [[CrossRef](#)]
42. Mohan, D.; Sarswat, A.; Ok, Y.S.; Pittman, C.U. Organic and Inorganic Contaminants Removal from Water with Biochar, a Renewable, Low Cost and Sustainable Adsorbent—A Critical Review. *Bioresour. Technol.* **2014**, *160*, 191–202. [[CrossRef](#)] [[PubMed](#)]
43. Gwenzi, W.; Chaukura, N.; Noubactep, C.; Mukome, F.N.D. Biochar-Based Water Treatment Systems as a Potential Low-Cost and Sustainable Technology for Clean Water Provision. *J. Environ. Manage.* **2017**, *197*, 732–749. [[CrossRef](#)]
44. Sizmur, T.; Fresno, T.; Akgül, G.; Frost, H.; Moreno-Jiménez, E. Biochar Modification to Enhance Sorption of Inorganics from Water. *Bioresour. Technol.* **2017**, *246*, 34–47. [[CrossRef](#)] [[PubMed](#)]
45. Tan, X.; Liu, Y.; Zeng, G.; Wang, X.; Hu, X.; Gu, Y.; Yang, Z. Application of Biochar for the Removal of Pollutants from Aqueous Solutions. *Chemosphere* **2015**, *125*, 70–85. [[CrossRef](#)] [[PubMed](#)]
46. Abbas, Z.; Ali, S.; Rizwan, M.; Zaheer, I.E.; Malik, A.; Riaz, M.A.; Shahid, M.R.; ur Rehman, M.Z.; Al-Wabel, M.I. A Critical Review of Mechanisms Involved in the Adsorption of Organic and Inorganic Contaminants through Biochar. *Arab. J. Geosci.* **2018**, *11*, 448. [[CrossRef](#)]
47. Ambaye, T.G.; van Hullebusch, M.V.E.D.; Rtimi, A.A.S. Mechanisms and Adsorption Capacities of Biochar for the Removal of Organic and Inorganic Pollutants from Industrial Wastewater. *Int. J. Environ. Sci. Technol.* **2021**, *18*, 3273–3294. [[CrossRef](#)]
48. Zeghioud, H.; Fryda, L.; Djelal, H.; Assadi, A.; Kane, A. A Comprehensive Review of Biochar in Removal of Organic Pollutants from Wastewater: Characterization, Toxicity, Activation/Functionalization and Influencing Treatment Factors. *J. Water Process Eng.* **2022**, *47*, 102801. [[CrossRef](#)]
49. Zhang, M.; Song, G.; Gelardi, D.L.; Huang, L.; Khan, E.; Mašek, O.; Parikh, S.J.; Ok, Y.S. Evaluating Biochar and Its Modifications for the Removal of Ammonium, Nitrate, and Phosphate in Water. *Water Res.* **2020**, *186*, 116303. [[CrossRef](#)]
50. Shakoob, M.B.; Ye, Z.L.; Chen, S. Engineered Biochars for Recovering Phosphate and Ammonium from Wastewater: A Review. *Sci. Total Environ.* **2021**, *779*, 146240. [[CrossRef](#)]
51. Almanassra, I.W.; McKay, G.; Kochkodan, V.; Ali Atieh, M.; Al-Ansari, T. A State of the Art Review on Phosphate Removal from Water by Biochars. *Chem. Eng. J.* **2021**, *409*, 128211. [[CrossRef](#)]
52. Ambika, S.; Kumar, M.; Pisharody, L.; Malhotra, M.; Kumar, G.; Sreedharan, V.; Singh, L.; Nidheesh, P.V.; Bhatnagar, A. Modified Biochar as a Green Adsorbent for Removal of Hexavalent Chromium from Various Environmental Matrices: Mechanisms, Methods, and Prospects. *Chem. Eng. J.* **2022**, *439*, 135716. [[CrossRef](#)]
53. Dai, Y.; Zhang, N.; Xing, C.; Cui, Q.; Sun, Q. The Adsorption, Regeneration and Engineering Applications of Biochar for Removal Organic Pollutants: A Review. *Chemosphere* **2019**, *223*, 12–27. [[CrossRef](#)] [[PubMed](#)]
54. Lakshmi, D.; Akhil, D.; Kartik, A.; Gopinath, K.P.; Arun, J.; Bhatnagar, A.; Rinklebe, J.; Kim, W.; Muthusamy, G. Artificial Intelligence (AI) Applications in Adsorption of Heavy Metals Using Modified Biochar. *Sci. Total Environ.* **2021**, *801*, 149623. [[CrossRef](#)]
55. Liu, T.; Lawluy, Y.; Shi, Y.; Ighalo, J.O.; He, Y.; Zhang, Y.; Yap, P.S. Adsorption of Cadmium and Lead from Aqueous Solution Using Modified Biochar: A Review. *J. Environ. Chem. Eng.* **2022**, *10*, 106502. [[CrossRef](#)]
56. Qiu, B.; Tao, X.; Wang, H.; Li, W.; Ding, X.; Chu, H. Biochar as a Low-Cost Adsorbent for Aqueous Heavy Metal Removal: A Review. *J. Anal. Appl. Pyrolysis* **2021**, *155*, 105081. [[CrossRef](#)]
57. Sharma, P.K.; Kumar, R.; Singh, R.K.; Sharma, P.; Ghosh, A. Review on Arsenic Removal Using Biochar-Based Materials. *Groundw. Sustain. Dev.* **2022**, *17*, 100740. [[CrossRef](#)]
58. Wang, L.; Wang, Y.; Ma, F.; Tankpa, V.; Bai, S.; Guo, X.; Wang, X. Mechanisms and Reutilization of Modified Biochar Used for Removal of Heavy Metals from Wastewater: A Review. *Sci. Total Environ.* **2019**, *668*, 1298–1309. [[CrossRef](#)]
59. Zheng, C.; Yang, Z.; Si, M.; Zhu, F.; Yang, W.; Zhao, F.; Shi, Y. Application of Biochars in the Remediation of Chromium Contamination: Fabrication, Mechanisms, and Interfering Species. *J. Hazard. Mater.* **2021**, *407*, 124376. [[CrossRef](#)]

60. Zoroufchi Benis, K.; Motalebi Damuchali, A.; Soltan, J.; McPhedran, K.N. Treatment of Aqueous Arsenic—A Review of Biochar Modification Methods. *Sci. Total Environ.* **2020**, *739*, 139750. [CrossRef]
61. Godwin, P.M.; Pan, Y.; Xiao, H.; Afzal, M.T. Progress in Preparation and Application of Modified Biochar for Improving Heavy Metal Ion Removal From Wastewater. *J. Bioresour. Bioprod.* **2019**, *4*, 31–42. [CrossRef]
62. Hussin, F.; Aroua, M.K.; Szlachta, M. Biochar Derived from Fruit By-Products Using Pyrolysis Process for the Elimination of Pb(II) Ion: An Updated Review. *Chemosphere* **2022**, *287*, 132250. [CrossRef] [PubMed]
63. Li, H.; Dong, X.; da Silva, E.B.; de Oliveira, L.M.; Chen, Y.; Ma, L.Q. Mechanisms of Metal Sorption by Biochars: Biochar Characteristics and Modifications. *Chemosphere* **2017**, *178*, 466–478. [CrossRef] [PubMed]
64. Berslin, D.; Reshmi, A.; Sivaprakash, B.; Rajamohan, N.; Kumar, P.S. Remediation of Emerging Metal Pollutants Using Environment Friendly Biochar- Review on Applications and Mechanism. *Chemosphere* **2022**, *290*, 133384. [CrossRef] [PubMed]
65. Cheng, N.; Wang, B.; Wu, P.; Lee, X.; Xing, Y.; Chen, M.; Gao, B. Adsorption of Emerging Contaminants from Water and Wastewater by Modified Biochar: A Review. *Environ. Pollut.* **2021**, *273*, 116448. [CrossRef]
66. Amusat, S.O.; Kebede, T.G.; Dube, S.; Nindi, M.M. Ball-Milling Synthesis of Biochar and Biochar-Based Nanocomposites and Prospects for Removal of Emerging Contaminants: A Review. *J. Water Process Eng.* **2021**, *41*, 101993. [CrossRef]
67. Shahid, M.K.; Kashif, A.; Fuwad, A.; Choi, Y. Current Advances in Treatment Technologies for Removal of Emerging Contaminants from Water—A Critical Review. *Coord. Chem. Rev.* **2021**, *442*, 213993. [CrossRef]
68. Biswal, B.K.; Vijayaraghavan, K.; Tsen-Tieng, D.L.; Balasubramanian, R. Biochar-Based Bioretention Systems for Removal of Chemical and Microbial Pollutants from Stormwater: A Critical Review. *J. Hazard. Mater.* **2022**, *422*, 126886. [CrossRef]
69. Hassan, M.; Liu, Y.; Naidu, R.; Parikh, S.J.; Du, J.; Qi, F.; Willett, I.R. Influences of Feedstock Sources and Pyrolysis Temperature on the Properties of Biochar and Functionality as Adsorbents: A Meta-Analysis. *Sci. Total Environ.* **2020**, *744*, 140714. [CrossRef]
70. Tomczyk, A.; Sokołowska, Z.; Boguta, P. Biochar Physicochemical Properties: Pyrolysis Temperature and Feedstock Kind Effects. *Rev. Environ. Sci. Bio/Technol.* **2020**, *19*, 191–215. [CrossRef]
71. Yang, H.; Yan, R.; Chen, H.; Lee, D.H.; Zheng, C. Characteristics of Hemicellulose, Cellulose and Lignin Pyrolysis. *Fuel* **2007**, *86*, 1781–1788. [CrossRef]
72. Yaashikaa, P.R.; Kumar, P.S.; Varjani, S.; Saravanan, A. A Critical Review on the Biochar Production Techniques, Characterization, Stability and Applications for Circular Bioeconomy. *Biotechnol. Rep.* **2020**, *28*, e00570. [CrossRef] [PubMed]
73. Wijitkosum, S. Biochar Derived from Agricultural Wastes and Wood Residues for Sustainable Agricultural and Environmental Applications. *Int. Soil Water Conserv. Res.* **2022**, *10*, 335–341. [CrossRef]
74. Ippolito, J.A.; Cui, L.; Kamman, C.; Wrage-Mönnig, N.; Estavillo, J.M.; Fuertes-Mendizabal, T.; Cayuela, M.L.; Sigua, G.; Novak, J.; Spokas, K.; et al. Feedstock Choice, Pyrolysis Temperature and Type Influence Biochar Characteristics: A Comprehensive Meta-Data Analysis Review. *Biochar* **2020**, *2*, 421–438. [CrossRef]
75. Enaime, G.; Baçaoui, A.; Yaacoubi, A.; Lübken, M. Biochar for Wastewater Treatment—Conversion Technologies and Applications. *Appl. Sci.* **2020**, *10*, 3492. [CrossRef]
76. Janu, R.; Mrlik, V.; Ribitsch, D.; Hofman, J.; Sedláček, P.; Bielská, L.; Soja, G. Biochar Surface Functional Groups as Affected by Biomass Feedstock, Biochar Composition and Pyrolysis Temperature. *Carbon Resour. Convers.* **2021**, *4*, 36–46. [CrossRef]
77. Zhang, Q.; Wang, Y.; Wang, Z.; Zhang, Z.; Wang, X.; Yang, Z. Active Biochar Support Nano Zero-Valent Iron for Efficient Removal of U(VI) from Sewage Water. *J. Alloy. Compd.* **2021**, *852*, 156993. [CrossRef]
78. Saleh, T.A.; Mustaqeem, M.; Khaled, M. Water Treatment Technologies in Removing Heavy Metal Ions from Wastewater: A Review. *Environ. Nanotechnol. Monit. Manag.* **2022**, *17*, 100617. [CrossRef]
79. Dulama, M.; Iordache, M.; Deneanu, N. Treatment of Uranium Contaminated Wastewater a review. In *Proceedings of NUCLEAR 2013 the 6th Annual International Conference on Sustainable Development through Nuclear Research and Education Part 3/3*; 2013; pp. 80–87. Available online: http://inis.iaea.org/search/search.aspx?orig_q=RN:47056986 (accessed on 22 October 2022).
80. Boraah, N.; Chakma, S.; Kaushal, P. Attributes of Wood Biochar as an Efficient Adsorbent for Remediating Heavy Metals and Emerging Contaminants from Water: A Critical Review and Bibliometric Analysis. *J. Environ. Chem. Eng.* **2022**, *10*, 107825. [CrossRef]
81. Sen, K.; Mishra, D.; Debnath, P.; Mondal, A.; Mondal, N.K. Adsorption of Uranium (VI) from Groundwater by Silicon Containing Biochar Supported Iron Oxide Nanoparticle. *Bioresour. Technol. Rep.* **2021**, *14*, 100659. [CrossRef]
82. Jin, J.; Li, S.; Peng, X.; Liu, W.; Zhang, C.; Yang, Y.; Han, L.; Du, Z.; Sun, K.; Wang, X. HNO₃ Modified Biochars for Uranium (VI) Removal from Aqueous Solution. *Bioresour. Technol.* **2018**, *256*, 247–253. [CrossRef]
83. Guo, Y.; Liu, X.; Xie, S.; Liu, H.; Wang, C.; Wang, L. 3D ZnO Modified Biochar-Based Hydrogels for Removing U(VI) in Aqueous Solution. *Colloids Surf. A Physicochem. Eng. Asp.* **2022**, *642*, 128606. [CrossRef]
84. Ioannou, K.; Hadjiyiannis, P.; Liatsou, I.; Pashalidis, I. U(VI) Adsorption by Biochar Fiber–MnO₂ Composites. *J. Radioanal. Nucl. Chem.* **2019**, *320*, 425–432. [CrossRef]
85. Lingamdinne, L.P.; Choi, J.S.; Angaru, G.K.R.; Karri, R.R.; Yang, J.K.; Chang, Y.Y.; Koduru, J.R. Magnetic-Watermelon Rinds Biochar for Uranium-Contaminated Water Treatment Using an Electromagnetic Semi-Batch Column with Removal Mechanistic Investigations. *Chemosphere* **2022**, *286*, 131776. [CrossRef] [PubMed]
86. Solanki, Y.S.; Agarwal, M.; Gupta, A.B.; Gupta, S.; Shukla, P. Fluoride Occurrences, Health Problems, Detection, and Remediation Methods for Drinking Water: A Comprehensive Review. *Sci. Total Environ.* **2022**, *807*, 150601. [CrossRef]

87. Nizam, S.; Virk, H.S.; Sen, I.S. High Levels of Fluoride in Groundwater from Northern Parts of Indo-Gangetic Plains Reveals Detrimental Fluorosis Health Risks. *Environ. Adv.* **2022**, *8*, 100200. [[CrossRef](#)]
88. Kashyap, S.J.; Sankannavar, R.; Madhu, G.M. Fluoride Sources, Toxicity and Fluorosis Management Techniques—A Brief Review. *J. Hazard. Mater. Lett.* **2021**, *2*, 100033. [[CrossRef](#)]
89. Zhou, N.; Guo, X.; Ye, C.; Yan, L.; Gu, W.; Wu, X.; Zhou, Q.; Yang, Y.; Wang, X.; Cheng, Q. Enhanced Fluoride Removal from Drinking Water in Wide PH Range Using La/Fe/Al Oxides Loaded Rice Straw Biochar. *Water Supply* **2022**, *22*, 779–794. [[CrossRef](#)]
90. Yan, L.; Gu, W.; Zhou, N.; Ye, C.; Yang, Y. Preparation and Characterization of Wheat Straw Biochar Loaded with Aluminium/Lanthanum Hydroxides: A Novel Adsorbent for Removing Fluoride from Drinking Water. *Environ. Technol.* **2021**, *43*, 2771–2784. [[CrossRef](#)]
91. Mohan, D.; Kumar, S.; Srivastava, A. Fluoride Removal from Ground Water Using Magnetic and Nonmagnetic Corn Stover Biochars. *Ecol. Eng.* **2014**, *73*, 798–808. [[CrossRef](#)]
92. Halder, G.; Khan, A.A.; Dhawane, S. Fluoride Sorption Onto a Steam-Activated Biochar Derived From Cocos Nucifera Shell. *CLEAN—Soil Air Water* **2016**, *44*, 124–133. [[CrossRef](#)]
93. Mei, L.; Qiao, H.; Ke, F.; Peng, C.; Hou, R.; Wan, X.; Cai, H. One-Step Synthesis of Zirconium Dioxide-Biochar Derived from Camellia Oleifera Seed Shell with Enhanced Removal Capacity for Fluoride from Water. *Appl. Surf. Sci.* **2020**, *509*, 144685. [[CrossRef](#)]
94. Sadhu, M.; Bhattacharya, P.; Vithanage, M.; Padmaja Sudhakar, P. Adsorptive Removal of Fluoride Using Biochar—A Potential Application in Drinking Water Treatment. *Sep. Purif. Technol.* **2022**, *278*, 119106. [[CrossRef](#)]
95. Wang, J.; Chen, N.; Li, M.; Feng, C. Efficient Removal of Fluoride Using Polypyrrole-Modified Biochar Derived from Slow Pyrolysis of Pomelo Peel: Sorption Capacity and Mechanism. *J. Polym. Environ.* **2018**, *26*, 1559–1572. [[CrossRef](#)]
96. Kumar, H.; Patel, M.; Mohan, D. Simplified Batch and Fixed-Bed Design System for Efficient and Sustainable Fluoride Removal from Water Using Slow Pyrolyzed Okra Stem and Black Gram Straw Biochars. *ACS Omega* **2019**, *4*, 19513–19525. [[CrossRef](#)]
97. Sha, Q.; Xie, H.; Liu, W.; Yang, D.; He, Y.; Yang, C.; Wang, N. Removal of Fluoride Using Platanus Acerifoli Leaves Biochar—An Efficient and Low-Cost Application in Wastewater Treatment. *Environ. Technol.* **2021**, 1–43. [[CrossRef](#)]
98. Jha, S.; Nanda, S.; Acharya, B.; Dalai, A.K. A Review of Thermochemical Conversion of Waste Biomass to Biofuels. *Energies* **2022**, *15*, 6352. [[CrossRef](#)]
99. Sun, Y.; Gao, B.; Yao, Y.; Fang, J.; Zhang, M.; Zhou, Y.; Chen, H.; Yang, L. Effects of Feedstock Type, Production Method, and Pyrolysis Temperature on Biochar and Hydrochar Properties. *Chem. Eng. J.* **2014**, *240*, 574–578. [[CrossRef](#)]
100. Tripathi, M.; Sahu, J.N.; Ganesan, P. Effect of Process Parameters on Production of Biochar from Biomass Waste through Pyrolysis: A Review. *Renew. Sustain. Energy Rev.* **2016**, *55*, 467–481. [[CrossRef](#)]
101. Asadi, H.; Ghorbani, M.; Rezaei-Rashti, M.; Abrishamkesh, S.; Amirahmadi, E.; Chengrong, C.; Gorji, M. Application of Rice Husk Biochar for Achieving Sustainable Agriculture and Environment. *Rice Sci.* **2021**, *28*, 325–343. [[CrossRef](#)]
102. Windeatt, J.H.; Ross, A.B.; Williams, P.T.; Forster, P.M.; Nahil, M.A.; Singh, S. Characteristics of Biochars from Crop Residues: Potential for Carbon Sequestration and Soil Amendment. *J. Environ. Manage.* **2014**, *146*, 189–197. [[CrossRef](#)] [[PubMed](#)]
103. Reguyal, F.; Sarmah, A.K.; Gao, W. Synthesis of Magnetic Biochar from Pine Sawdust via Oxidative Hydrolysis of FeCl₂ for the Removal Sulfamethoxazole from Aqueous Solution. *J. Hazard. Mater.* **2017**, *321*, 868–878. [[CrossRef](#)] [[PubMed](#)]
104. Umar, M.; Amru, A.R.; Amin, N.H.M.; Zaid, H.M.; Guan, B.H. Biomass Activated Carbon from Oil Palm Shell as Potential Material to Control Filtration Loss in Water-Based Drilling Fluid. *Optim. Based Model Using Fuzzy Other Stat. Tech. Towar. Environ. Sustain.* **2020**, 55–65.
105. Hu, H.; Zhang, X.; Wang, T.; Sun, L.; Wu, H.; Chen, X. Bamboo (*Acidosasa longiligula*) Shoot Shell Biochar: Its Potential Application to Isolation of Uranium(VI) from Aqueous Solution. *J. Radioanal. Nucl. Chem.* **2018**, *316*, 349–362. [[CrossRef](#)]
106. Ying, D.; Hong, P.; Jiali, F.; Qinqin, T.; Yuhui, L.; Youqun, W.; Zhibin, Z.; Xiaohong, C.; Yunhai, L. Removal of Uranium Using MnO₂/Orange Peel Biochar Composite Prepared by Activation and in-Situ Deposit in a Single Step. *Biomass Bioenergy* **2020**, *142*, 105772. [[CrossRef](#)]
107. Liao, J.; Ding, L.; Zhang, Y.; Zhu, W. Efficient Removal of Uranium from Wastewater Using Pig Manure Biochar: Understanding Adsorption and Binding Mechanisms. *J. Hazard. Mater.* **2022**, *423*, 127190. [[CrossRef](#)]
108. Liao, J.; He, X.; Zhang, Y.; Zhu, W.; Zhang, L.; He, Z. Bismuth Impregnated Biochar for Efficient Uranium Removal from Solution: Adsorption Behavior and Interfacial Mechanism. *Sci. Total Environ.* **2022**, *819*, 153145. [[CrossRef](#)]
109. Wallace, A.R.; Su, C.; Choi, Y.-K.; Kan, E.; Sun, W. Removal of Fluoride from Water Using a Calcium-Modified Dairy Manure-Derived Biochar. *J. Environ. Eng.* **2020**, *146*, 1–10. [[CrossRef](#)]
110. Xu, D.; Fan, X.; Chen, Q.; Qiao, S.; Zhang, J.; Yang, Y.; Wang, H.; Zhang, L.; Hou, J. Removal of Nitrogen and Phosphorus from Water by Sludge-Based Biochar Modified by Montmorillonite Coupled with Nano Zero-Valent Iron. *Water Sci. Technol.* **2022**, *85*, 2114–2128. [[CrossRef](#)]
111. Hu, R.; Xiao, J.; Wang, T.; Chen, G.; Chen, L.; Tian, X. Engineering of Phosphate-Functionalized Biochars with Highly Developed Surface Area and Porosity for Efficient and Selective Extraction of Uranium. *Chem. Eng. J.* **2020**, *379*, 122388. [[CrossRef](#)]
112. Alkurdi, S.S.A.; Al-juboori, R.A.; Bundschuh, J.; Bowtell, L. Effect of Pyrolysis Conditions on Bone Char Characterization and Its Ability for Arsenic and Fluoride Removal. *Environ. Pollut.* **2020**, *262*, 114221. [[CrossRef](#)] [[PubMed](#)]

113. Thúy, N.; Chi, L.; Anto, S.; Shan, T.; Kumar, S.S.; Shanmugam, S.; Samuel, M.S.; Mathimani, T.; Brindhadevi, K.; Pugazhendhi, A. A Review on Biochar Production Techniques and Biochar Based Catalyst for Biofuel Production from Algae. *Fuel* **2020**, *287*, 119411. [CrossRef]
114. Gabhane, J.W.; Bhange, V.P.; Patil, P.D.; Bankar, S.T.; Kumar, S. Recent Trends in Biochar Production Methods and Its Application as a Soil Health Conditioner: A Review. *SN Appl. Sci.* **2020**, *2*, 1307. [CrossRef]
115. Wang, J.; Wang, S. Preparation, Modification and Environmental Application of Biochar: A Review. *J. Clean. Prod.* **2019**, *227*, 1002–1022. [CrossRef]
116. Chen, D.; Zheng, Z.; Fu, K.; Zeng, Z.; Wang, J.; Lu, M. Torrefaction of Biomass Stalk and Its Effect on the Yield and Quality of Pyrolysis Products. *Fuel* **2015**, *159*, 27–32. [CrossRef]
117. Heidenreich, S.; Müller, M.; Foscolo, P.U. Chapter 3—Biomass Pretreatment. In *Advanced biomass gasification*; Heidenreich, S., Müller, M., Foscolo, P.U.B.T.-A.B.G., Eds.; Academic Press: Cambridge, MA, USA, 2016; pp. 11–17. ISBN 978-0-12-804296-0. Available online: <https://www.sciencedirect.com/science/article/pii/B978012804296000038> (accessed on 22 October 2022).
118. Hadjittofi, L.; Pashalidis, I. Uranium Sorption from Aqueous Solutions by Activated Biochar Fibres Investigated by FTIR Spectroscopy and Batch Experiments. *J. Radioanal. Nucl. Chem.* **2015**, *304*, 897–904. [CrossRef]
119. Liatsou, I.; Michail, G.; Demetriou, M.; Pashalidis, I. Uranium Binding by Biochar Fibres Derived from *Luffa Cylindrica* after Controlled Surface Oxidation. *J. Radioanal. Nucl. Chem.* **2017**, *311*, 871–875. [CrossRef]
120. Paschalidou, P.; Pashalidis, I.; Manariotis, I.D.; Karapanagioti, H.K. Hyper Sorption Capacity of Raw and Oxidized Biochars from Various Feedstocks for U(VI). *J. Environ. Chem. Eng.* **2020**, *8*, 103932. [CrossRef]
121. Stasi, C.; Georgiou, E.; Ioannidis, I.; Pashalidis, I. Uranium Removal from Laboratory and Environmental Waters by Oxidised Biochar Prepared from Palm Tree Fibres. *J. Radioanal. Nucl. Chem.* **2022**, *331*, 375–381. [CrossRef]
122. Xia, D.; Liu, Y.; Cheng, X.; Gu, P.; Chen, Q.; Zhang, Z. Applied Surface Science Temperature-Tuned Fish-Scale Biochar with Two-Dimensional Homogeneous Porous Structure: A Promising Uranium Extractant. *Appl. Surf. Sci.* **2022**, *591*, 153136. [CrossRef]
123. Saikia, R.; Goswami, R.; Bordoloi, N.; Senapati, K.K.; Pant, K.K.; Kumar, M.; Katak, R. Removal of Arsenic and Fluoride from Aqueous Solution by Biomass Based Activated Biochar: Optimization through Response Surface Methodology. *J. Environ. Chem. Eng.* **2017**, *5*, 5528–5539. [CrossRef]
124. Han, L.; Zhang, E.; Yang, Y.; Sun, K.; Fang, L. Highly Efficient U(VI) Removal by Chemically Modified Hydrochar and Pyrochar Derived from Animal Manure. *J. Clean. Prod.* **2020**, *264*, 121542. [CrossRef]
125. Li, M.; Liu, H.; Chen, T.; Dong, C.; Sun, Y. Synthesis of Magnetic Biochar Composites for Enhanced Uranium(VI) Adsorption. *Sci. Total Environ.* **2019**, *651*, 1020–1028. [CrossRef] [PubMed]
126. Liao, J.; Xiong, T.; Ding, L.; Zhang, Y.; Zhu, W. Effective Separation of Uranium(VI) from Wastewater Using a Magnetic Carbon as a Recyclable Adsorbent. *Sep. Purif. Technol.* **2022**, *282*, 120140. [CrossRef]
127. Ding, L.; Tan, W.; Xie, S.; Mumford, K.; Lv, J.; Wang, H.; Fang, Q.; Zhang, X.; Wu, X.; Li, M. Uranium Adsorption and Subsequent Re-Oxidation under Aerobic Conditions by *Leifsonia* sp.—Coated Biochar as Green Trapping Agent. *Environ. Pollut.* **2018**, *242*, 778–787. [CrossRef] [PubMed]
128. Wei, Y.; Wang, L.; Wang, J. Cerium Alginate Cross-Linking with Biochar Beads for Fast Fluoride Removal over a Wide PH Range. *Colloids Surf. A Physicochem. Eng. Asp.* **2022**, *636*, 128161. [CrossRef]
129. An, Q.; Li, X.Q.; Nan, H.Y.; Yu, Y.; Jiang, J.N. The Potential Adsorption Mechanism of the Biochars with Different Modification Processes to Cr(VI). *Environ. Sci. Pollut. Res.* **2018**, *25*, 31346–31357. [CrossRef]
130. Chemerys, V.; Baltreñaitė, E. Modified Biochar: A Review on Modifications of Biochar Towards Its Enhanced Adsorptive Properties. 2016.
131. Ahmed, W.; Núñez-Delgado, A.; Mehmood, S.; Ali, S.; Qaswar, M.; Shakoore, A.; Chen, D.Y. Highly Efficient Uranium (VI) Capture from Aqueous Solution by Means of a Hydroxyapatite-Biochar Nanocomposite: Adsorption Behavior and Mechanism. *Environ. Res.* **2021**, *201*, 111518. [CrossRef]
132. Wang, S.; Guo, W.; Gao, F.; Wang, Y.; Gao, Y. Lead and Uranium Sorptive Removal from Aqueous Solution Using Magnetic and Nonmagnetic Fast Pyrolysis Rice Husk Biochars. *RSC Adv.* **2018**, *8*, 13205–13217. [CrossRef]
133. Chen, W.; Feng, J.; Liu, S.; Zhang, J.; Cai, Y.; Lv, Z.; Fang, M.; Tan, X. A Green and Economical MgO/Biochar Composite for the Removal of U(VI) from Aqueous Solutions. *Chem. Eng. Res. Des.* **2022**, *180*, 391–401. [CrossRef]
134. Lyu, P.; Wang, G.; Wang, B.; Yin, Q.; Li, Y.; Deng, N. Adsorption and Interaction Mechanism of Uranium (VI) from Aqueous Solutions on Phosphate-Impregnation Biochar Cross-Linked MgAl Layered Double-Hydroxide Composite. *Appl. Clay Sci.* **2021**, *209*, 106146. [CrossRef]
135. Li, N.; Yin, M.; Tsang, D.C.W.; Yang, S.; Liu, J.; Li, X.; Song, G.; Wang, J. Mechanisms of U(VI) Removal by Biochar Derived from *Ficus Microcarpa* Aerial Root: A Comparison between Raw and Modified Biochar. *Sci. Total Environ.* **2019**, *697*, 134115. [CrossRef]
136. Hu, Q.; Zhu, Y.; Hu, B.; Lu, S.; Sheng, G. Mechanistic Insights into Sequestration of U (VI) toward Magnetic Biochar: Batch, XPS and EXAFS Techniques. *J. Environ. Sci.* **2018**, *70*, 217–225. [CrossRef] [PubMed]
137. Zhou, Y.; Xiao, J.; Hu, R.; Wang, T.; Shao, X.; Chen, G.; Chen, L.; Tian, X. Engineered Phosphorous-Functionalized Biochar with Enhanced Porosity Using Phytic Acid-Assisted Ball Milling for Efficient and Selective Uptake of Aquatic Uranium. *J. Mol. Liq.* **2020**, *303*, 112659. [CrossRef]

138. Liao, J.; Chen, H.; Zhang, Y.; Zhu, W. Pyrolysis of Animal Manure under Nitrogen Atmosphere: An Environment Protection Way to Obtain Animal Manure Biochar for High-Efficient Adsorption of Uranium (VI). *J. Anal. Appl. Pyrolysis* **2022**, *163*, 105493. [[CrossRef](#)]
139. Zheng, B.; Liao, J.; Ding, L.; Zhang, Y.; Zhu, W. High Efficiency Adsorption of Uranium in Solution with Magnesium Oxide Embedded Horse Manure-Derived Biochar. *J. Environ. Chem. Eng.* **2021**, *9*, 106897. [[CrossRef](#)]
140. Sun, Y.; Zeng, B.; Dai, Y.; Liang, X.; Zhang, L.; Ahmad, R.; Su, X. Modification of Sludge-Based Biochar Using Air Roasting-Oxidation and Its Performance in Adsorption of Uranium(VI) from Aqueous Solutions. *J. Colloid Interface Sci.* **2022**, *614*, 547–555. [[CrossRef](#)]
141. Noli, F.; Kapashi, E.; Pashalidis, I.; Margellou, A.; Karfaridis, D. The Effect of Chemical and Thermal Modifications on the Biosorption of Uranium in Aqueous Solutions Using Winery Wastes. *J. Mol. Liq.* **2022**, *351*, 118665. [[CrossRef](#)]
142. Pang, H.; Diao, Z.; Wang, X.; Ma, Y.; Yu, S.; Zhu, H.; Chen, Z.; Hu, B.; Chen, J.; Wang, X. Adsorptive and Reductive Removal of U(VI) by Dictyophora Indusiate-Derived Biochar Supported Sulfide NZVI from Wastewater. *Chem. Eng. J.* **2019**, *366*, 368–377. [[CrossRef](#)]
143. Wang, B.; Zheng, J.; Li, Y.; Zaidi, A.; Hu, Y.; Hu, B. Fabrication of δ -MnO₂-Modified Algal Biochar for Efficient Removal of U(VI) from Aqueous Solutions. *J. Environ. Chem. Eng.* **2021**, *9*, 105625. [[CrossRef](#)]
144. Wang, B.; Li, Y.; Zheng, J.; Hu, Y.; Wang, X.; Hu, B. Efficient Removal of U(VI) from Aqueous Solutions Using the Magnetic Biochar Derived from the Biomass of a Bloom-Forming Cyanobacterium (*Microcystis aeruginosa*). *Chemosphere* **2020**, *254*, 126898. [[CrossRef](#)] [[PubMed](#)]
145. Liatsou, I.; Pashalidis, I.; Nicolaidis, A. Triggering Selective Uranium Separation from Aqueous Solutions by Using Salophen-Modified Biochar Fibers. *J. Radioanal. Nucl. Chem.* **2018**, *318*, 2199–2203. [[CrossRef](#)]
146. Ye, T.; Huang, B.; Wang, Y.; Zhou, L.; Liu, Z. Rapid Removal of Uranium(VI) Using Functionalized Luffa Rattan Biochar from Aqueous Solution. *Colloids Surf. A Physicochem. Eng. Asp.* **2020**, *606*, 125480. [[CrossRef](#)]
147. Akl, Z.F.; Zaki, E.G.; ElSaeed, S.M. Green Hydrogel-Biochar Composite for Enhanced Adsorption of Uranium. *ACS Omega* **2021**, *6*, 34193–34205. [[CrossRef](#)] [[PubMed](#)]
148. Liu, J.; Ge, Y.; Wang, G.; Liu, Y.; Xu, X. Highly Efficient Removal of U(VI) in Aqueous Solutions by Tea Waste-Derived Biochar-Supported Iron-Manganese Oxide Composite. *J. Radioanal. Nucl. Chem.* **2021**, *330*, 871–882. [[CrossRef](#)]
149. Yadav, K.; Jagadevan, S. Effect of Pyrolysis of Rice Husk-Derived Biochar on the Fuel Characteristics and Adsorption of Fluoride from Aqueous Solution. *Bioenergy Res.* **2021**, *14*, 964–977. [[CrossRef](#)]
150. Shen, Z.; Jin, J.; Fu, J.; Yang, M.; Li, F. Anchoring Al- and/or Mg-Oxides to Magnetic Biochars for Co-Uptake of Arsenate and Fluoride from Water. *J. Environ. Manage.* **2021**, *293*, 112898. [[CrossRef](#)]
151. Yadav, T.K.; Abhishek; Prasad, B.; Singh, D.; Prasad, K.S. Calcium Pretreated Pinus Roxburghii Wood Biochar for Adsorptive Removal of Fluoride from Aqueous Solution. *Biointerface Res. Appl. Chem.* **2022**, *12*, 4307–4316. [[CrossRef](#)]
152. Bombuwala Dewage, N.; Liyanage, A.S.; Pittman, C.U.; Mohan, D.; Mlsna, T. Fast Nitrate and Fluoride Adsorption and Magnetic Separation from Water on A-Fe₂O₃ and Fe₃O₄ Dispersed on Douglas Fir Biochar. *Bioresour. Technol.* **2018**, *263*, 258–265. [[CrossRef](#)]
153. Herath, A.; Navarathna, C.; Warren, S.; Perez, F.; Pittman, C.U.; Mlsna, T.E. Iron/Titanium Oxide-Biochar (Fe₂TiO₅/BC): A Versatile Adsorbent/Photocatalyst for Aqueous Cr(VI), Pb²⁺, F⁻ and Methylene Blue. *J. Colloid Interface Sci.* **2022**, *614*, 603–616. [[CrossRef](#)]
154. Rupasinghe, N.K.L.C.; Senanayake, S.M.A.E.; Nanayakkara, K.G.N. Development, Characterization and Mechanisms Study of Protonated Sawdust Biochar-Chitosan Composite Bead Biosorbent for Defluoridation of Contaminated Groundwater. *Bioresour. Technol. Rep.* **2022**, *17*, 100946. [[CrossRef](#)]
155. Wan, S.; Lin, J.; Tao, W.; Yang, Y.; Li, Y.; He, F. Enhanced Fluoride Removal from Water by Nanoporous Biochar-Supported Magnesium Oxide. *Ind. Eng. Chem. Res.* **2019**, *58*, 9988–9996. [[CrossRef](#)]
156. Meilani, V.; Lee, J.I.; Kang, J.K.; Lee, C.G.; Jeong, S.; Park, S.J. *Application of Aluminum-Modified Food Waste Biochar as Adsorbent of Fluoride in Aqueous Solutions and Optimization of Production Using Response Surface Methodology*; Elsevier Inc.: Amsterdam, The Netherlands, 2021; Volume 312, ISBN 0003212254. [[CrossRef](#)]
157. Roy, S.; Sengupta, S.; Manna, S.; Das, P. Chemically Reduced Tea Waste Biochar and Its Application in Treatment of Fluoride Containing Wastewater: Batch and Optimization Using Response Surface Methodology. *Process Saf. Environ. Prot.* **2018**, *116*, 553–563. [[CrossRef](#)]
158. Naga Babu, A.; Srinivasa Reddy, D.; Suresh Kumar, G.; Ravindhranath, K.; Krishna Mohan, G.V. Sequential Synergetic Sorption Analysis of Gracilaria Rhodophyta Biochar toward Aluminum and Fluoride: A Statistical Optimization Approach. *Water Environ. Res.* **2020**, *92*, 880–898. [[CrossRef](#)]
159. Ashraf, I.; Li, R.; Chen, B.; Al-Ansari, N.; Rizwan Aslam, M.; Altaf, A.R.; Elbeltagi, A. Nanoarchitectonics and Kinetics Insights into Fluoride Removal from Drinking Water Using Magnetic Tea Biochar. *Int. J. Environ. Res. Public Health* **2022**, *19*, 13092. [[CrossRef](#)]
160. Kumar, P.; Prajapati, A.K.; Dixit, S.; Yadav, V.L. Adsorption of Fluoride from Aqueous Solution Using Biochar Prepared from Waste Peanut Hull. *Mater. Res. Express* **2019**, *6*, 125553. [[CrossRef](#)]
161. Khan, B.A.; Ahmad, M.; Iqbal, S.; Bolan, N.; Zubair, S.; Shafique, M.A.; Shah, A. Effectiveness of the Engineered Pinecone-Derived Biochar for the Removal of Fluoride from Water. *Environ. Res.* **2022**, *212*, 113540. [[CrossRef](#)]

162. Papari, F.; Najafabadi, P.R.; Ramavandi, B. Fluoride Ion Removal from Aqueous Solution, Groundwater, and Seawater by Granular and Powdered *Conocarpus Erectus* Biochar. *Desalin. Water Treat.* **2017**, *65*, 375–386. [[CrossRef](#)]
163. Chunhui, L.; Jin, T.; Puli, Z.; Bin, Z.; Duo, B.; Xuebin, L. Simultaneous Removal of Fluoride and Arsenic in Geothermal Water in Tibet Using Modified Yak Dung Biochar as an Adsorbent. *R. Soc. Open Sci.* **2018**, *5*, 181266. [[CrossRef](#)]
164. Sajjadi, B.; Chen, W.Y.; Egiebor, N.O. A Comprehensive Review on Physical Activation of Biochar for Energy and Environmental Applications. *Rev. Chem. Eng.* **2019**, *35*, 735–776. [[CrossRef](#)]
165. Zhao, F.; Shan, R.; Gu, J.; Zhang, Y.; Yuan, H.; Chen, Y. Magnetically Recyclable Loofah Biochar by KMnO₄ Modification for Adsorption of Cu(II) from Aqueous Solutions. *ACS Omega* **2022**, *7*, 8844–8853. [[CrossRef](#)]
166. Zhai, W.; Sakthivel, T.; Chen, F.; Du, C.; Yu, H.; Dai, Z. Amorphous Materials for Elementary-Gas-Involved Electrocatalysis: An Overview. *Nanoscale* **2021**, *13*, 19783–19811. [[CrossRef](#)]
167. Su, M.; Tsang, D.C.W.; Ren, X.; Shi, Q.; Tang, J.; Zhang, H.; Kong, L.; Hou, L.; Song, G.; Chen, D. Removal of U(VI) from Nuclear Mining Effluent by Porous Hydroxyapatite: Evaluation on Characteristics, Mechanisms and Performance. *Environ. Pollut.* **2019**, *254*, 112891. [[CrossRef](#)]
168. Wang, X.; Guo, Z.; Hu, Z.; Zhang, J. Recent Advances in Biochar Application for Water and Wastewater Treatment: A Review. *PeerJ* **2020**, *8*, e9164. [[CrossRef](#)]
169. Mühr-Ebert, E.L.; Wagner, F.; Walther, C. Speciation of Uranium: Compilation of a Thermodynamic Database and Its Experimental Evaluation Using Different Analytical Techniques. *Appl. Geochem.* **2019**, *100*, 213–222. [[CrossRef](#)]
170. Kumar, A.; Tripathi, R.M.; Rout, S.; Mishra, M.K.; Ravi, P.M.; Ghosh, A.K. Characterization of Groundwater Composition in Punjab State with Special Emphasis on Uranium Content, Speciation and Mobility. *Radiochim. Acta* **2014**, *102*, 239–254. [[CrossRef](#)]
171. Tan, Z.; Yuan, S.; Hong, M.; Zhang, L.; Huang, Q. Mechanism of Negative Surface Charge Formation on Biochar and Its Effect on the Fixation of Soil Cd. *J. Hazard. Mater.* **2020**, *384*, 121370. [[CrossRef](#)]
172. Zhang, Z.B.; Cao, X.H.; Liang, P.; Liu, Y.H. Adsorption of Uranium from Aqueous Solution Using Biochar Produced by Hydrothermal Carbonization. *J. Radioanal. Nucl. Chem.* **2013**, *295*, 1201–1208. [[CrossRef](#)]
173. Li, X.; Pan, H.; Yu, M.; Wakeel, M.; Luo, J.; Alharbi, N.S.; Liao, Q.; Liu, J. Macroscopic and Molecular Investigations of Immobilization Mechanism of Uranium on Biochar: EXAFS Spectroscopy and Static Batch. *J. Mol. Liq.* **2018**, *269*, 64–71. [[CrossRef](#)]
174. Albayari, M.; Nazal, M.K.; Khalili, F.I.; Nordin, N.; Adnan, R. Biochar Derived from *Salvadora Persica* Branches Biomass as Low-Cost Adsorbent for Removal of Uranium(VI) and Thorium(IV) from Water. *J. Radioanal. Nucl. Chem.* **2021**, *328*, 669–678. [[CrossRef](#)]
175. Mishra, V.; Sureshkumar, M.K.; Gupta, N.; Kaushik, C.P. Study on Sorption Characteristics of Uranium onto Biochar Derived from Eucalyptus Wood. *Water. Air. Soil Pollut.* **2017**, *228*, 309. [[CrossRef](#)]
176. Xu, Z.; Xing, Y.; Ren, A.; Ma, D.; Li, Y.; Hu, S. Study on Adsorption Properties of Water Hyacinth-Derived Biochar for Uranium (VI). *J. Radioanal. Nucl. Chem.* **2020**, *324*, 1317–1327. [[CrossRef](#)]
177. Kumar, S.; Loganathan, V.A.; Gupta, R.B.; Barnett, M.O. An Assessment of U(VI) Removal from Groundwater Using Biochar Produced from Hydrothermal Carbonization. *J. Environ. Manage.* **2011**, *92*, 2504–2512. [[CrossRef](#)]
178. Yadav, K.; Jagadevan, S. Influence of Torrefaction and Pyrolysis on Engineered Biochar and Its Applicability in Defluoridation: Insight into Adsorption Mechanism, Batch Adsorber Design and Artificial Neural Network Modelling. *J. Anal. Appl. Pyrolysis.* **2021**, *154*, 105015. [[CrossRef](#)]
179. Mohan, D.; Sharma, R.; Singh, V.K.; Steele, P.; Pittman, C.U. Fluoride Removal from Water Using Bio-Char, a Green Waste, Low-Cost Adsorbent: Equilibrium Uptake and Sorption Dynamics Modeling. *Ind. Eng. Chem. Res.* **2012**, *51*, 900–914. [[CrossRef](#)]
180. Dong, Q.; Yang, D.; Luo, L.; He, Q.; Cai, F.; Cheng, S.; Chen, Y. Engineering Porous Biochar for Capacitive Fluorine Removal. *Sep. Purif. Technol.* **2021**, *257*, 117932. [[CrossRef](#)]
181. Shahid, M.K.; Kim, J.Y.; Shin, G.; Choi, Y. Effect of Pyrolysis Conditions on Characteristics and Fluoride Adsorptive Performance of Bone Char Derived from Bone Residue. *J. Water Process Eng.* **2020**, *37*, 101499. [[CrossRef](#)]
182. Mahmoud, M.E.; Khalifa, M.A.; El Wakeel, Y.M.; Header, M.S.; El-Sharkawy, R.M.; Kumar, S.; Abdel-Fattah, T.M. A Novel Nanocomposite of Liquidambar Styraciflua Fruit Biochar-Crosslinked-Nanosilica for Uranium Removal from Water. *Bioresour. Technol.* **2019**, *278*, 124–129. [[CrossRef](#)]
183. Ahmed, N.; Rahman, M.; Won, S.; Shim, S. Biochar Properties and Eco-Friendly Applications for Climate Change Mitigation, Waste Management, and Wastewater Treatment: A Review. *Renew. Sustain. Energy Rev.* **2017**, *79*, 255–273. [[CrossRef](#)]
184. Kumar, R.; Sharma, P.; Yang, W.; Sillanpää, M.; Shang, J.; Bhattacharya, P.; Vithanage, M.; Maity, J.P. State-of-the-Art of Research Progress on Adsorptive Removal of Fluoride-Contaminated Water Using Biochar-Based Materials: Practical Feasibility through Reusability and Column Transport Studies. *Environ. Res.* **2022**, *214*, 114043. [[CrossRef](#)]
185. Wang, J.; Chen, N.; Feng, C.; Li, M. Performance and Mechanism of Fluoride Adsorption from Groundwater by Lanthanum-Modified Pomelo Peel Biochar. *Environ. Sci. Pollut. Res.* **2018**, *25*, 15326–15335. [[CrossRef](#)]
186. Zhou, J.; Liu, Y.; Han, Y.; Jing, F.; Chen, J. Bone-Derived Biochar and Magnetic Biochar for Effective Removal of Fluoride in Groundwater: Effects of Synthesis Method and Coexisting Chromium. *Water Environ. Res.* **2019**, *91*, 588–597. [[CrossRef](#)]
187. Mandoreba, C.; Gwenzi, W.; Chaukura, N. Defluoridation of Drinking Water Using a Ceramic Filter Decorated with Iron Oxide-Biochar Composites. *Int. J. Appl. Ceram. Technol.* **2021**, *18*, 1321–1329. [[CrossRef](#)]